A PITCH OF SPIRAL
(The Laboratory History with a Preface and an Epilogue)

V.P. Plakhty

Preface

"In the beginning was the Word" [1]. When graduated from the Polytechnic in the April 1962 I had appeared in front of G.A. Smolensky, a head of the Laboratory of Magnetism and Ferroelectricity in the late Institute for Semiconductors of Academy of Sciences of the late USSR, he actually said a little more than one Word: "You will do neutrons at Gatchina." That time there were three condensed-matter instruments at the reactor: the polarised-neutron beam-line where G.M. Drabkin with his team made the first experiments with polarised neutrons, the time-of-flight spectrometer (a property of the Institute for Semiconductors) and the powder diffractometer (a property of the Moscow Institute for Crystallography) that was occasionally used by a thesis student. When my boss at Gatchina, G.M. Drabkin, had realized that my first boss was going to invest in these neutrons only my salary of 83 roubles per month (the lowest one of a senior technician in the Academy of Sciences) he decided that this is not enough to get one beam-tube more and that I should join E.I. Maltzev who was responsible for the diffractometer.

Together we have found a superstructure in $BiFeO_3$, the substance studied before by R.P. Ozerov, and I have understood forever that any new result needs an advantage in the experimental technique [2]. Unfortunately this was the first and the last experiment on this instrument, and mainly due to political reasons we spent five years of our life for the machinery with no financial investment. Nevertheless before 1971 eight papers were published including one on the neutron diffraction study of a manganate system $CaMnO_3 - BiMnO_3$. At present the manganates are the most popular systems in the solid-state physics. In spite of this I consider as more important our publication with W. Cochran on the X-ray scattering by a phonon soft mode in the lanthanum aluminate [3]. This was the first observation of the soft mode with a non-zero wave vector. The soft-mode mechanism proposed by W. Cochran is now known to be

G.M. Drabkin when bossing our group. From left to right:
O.P. Smirnov, V.A. Kudryashev, I.V. Golosovsky, V.P. Plakhty

responsible for the majority of the second order (or nearly second order) phase transitions. To the moment when a Division of the Ioffe Institute in Gatchina had been transformed into the Konstantinov Leningrad Nuclear Physics Institute I was employed there and worked in the group, the members of which one can see in photo together with our boss who can be recognized without any explanation. This was an embryo of our present laboratory.

V.I. Sokolov, 1986

The feature of our group (laboratory) is our specialization. Having only the neutron (X-ray) scattering, we were always able to investigate microscopic mechanisms of solid-state phenomena, which is good, without a possibility of studying the macroscopic properties due to these phenomena, which is very bad. We had neither macroscopic methods nor a chemical basis for the synthesis of new materials and for the crystal growing. In this situation we had to find the groups that had got these possibilities and were ideologically close to us. For the historical reasons we collaborated from the very beginning with the laboratory of G.A. Smolensky. But most of all we had fruitful contacts with the group of V.I. Sokolov from Moscow State University. We had met at the Low-Temperature Conference in Donetzk in 1973 to become friends the next day and forever. We had very similar sights on physics and on the life in general. Together we made many works using our joint experimental possibilities and the same crystals of excellent quality, which were grown by B.V. Mill. Even now, almost 30 years after our first contact I come back from time to time to the subjects, which we had started together.

I believe that two people had created the laboratory. G.A. Smolensky who said the Words, and G.M. Drabkin who supervised us nearly for 20 years. Very important were the permanent communications with A.S. Borovik-Romanov, whose seminar was for us the highest judgement.

G.A. Smolensky, July 1984

A.S. Borovik-Romanov, July 1984

I have decided to make this paper not very formalized. This is supposed to be a sort of memoirs with some cases from our life mixed with a purely scientific report. As there is no possibility to give in detail everything that was done during 30 years, I present as separate sections the main results and directions of our activity, which have normally ended in theses. The last section “Miscellaneous” is devoted to the works, which are not that important or have not finished yet to make a separate section. I estimate that nearly a half of our activities and about one third of the publication list are presented.

Scientific activities during 30 years A.D.

1. ***Magnetically diluted ferrimagnets and the bond percolation***

Apparently the first studied by neutron diffraction in the independent Leningrad Nuclear Physics Institute were the ferrimagnets with the garnet structure, in which one sublattice was magnetically diluted. The garnet general formula is $\{M1\}_3[M2]_2(M3)_3O_{12}$ with metal ions $M1$, $M2$ and $M3$ in three types of the oxygen coordination: dodecahedral (c), octahedral (a) and tetrahedral (d), respectively. The most known is the yttrium-iron garnet $Y_3Fe_2Fe_3O_{12}$ [4], in which the a- and the d-sublattices have the opposite orientation of the Fe^{3+} spins (S = 5/2), and this ferrite is a ferrimagnet with a spontaneous moment of about 5 μ_B. This ferrimagnet has very narrow width of the ferromagnetic resonance and, as a consequence, very high efficiency in the ultra-high frequency technique. Trying to substitute expensive yttrium by something else, one inevitably substituted Fe^{3+} either in the octahedral or in the tetrahedral sites by a non-magnetic ion. At low concentration, x, of the magnetic atoms the spontaneous moment, m, in both cases vanishes. It was generally believed that this occurs at $x = 0$. We have first observed [5] that m becomes zero far from $x = 0$.

Broadbent and Hammersley [6] had considered a mathematical model for a periodic network of valves (sites) connected by the tubes (bonds) and supplied in an arbitrary point by liquid. At some critical number of statistically opened sites (bonds) the liquid spreads (percolates) to the infinity. Two problems were studied: a site percolation with all tubes open and a bond percolation with all valves open. Domb and Sykes [7] have observed that a diluted ferromagnet is an analogue of the site percolation. In other words at a critical concentration of magnetic atoms (percolation limit) finite magnetic clusters are united in the infinite one. We have proposed that a ferrimagnet with one magnetically diluted sublattice has an analogue in the bond percolation as far as one sublattice creates bonds for the other one. The percolation limit that depends on the spatial dimensionality and on the number of bonds occurred to be in a good agreement $p_a = 0.39(1)$ and $p_d = 0.25(1)$ with the experimental critical concentrations $x_a = 0.40(2)$ and $x_d = 0.25(2)$ of magnetic atoms in the diluted octahedral and tetrahedral sublattices, which make bonds for the tetrahedral ($z = 4$) and the octahedral ($z = 6$) sublattices, respectively. I would like to mention a funny story on the translation procedure. That time I have not found a proper word in Russian and translated “percolation” as something like “sweeping through”. Afterwards I was very surprised to find out in the English version of our paper a word “filtration” instead of “percolation”, which was completely incomprehensible. Now the “percolation” is used in the Russian-language scientific literature as well. These investigations had made a basis of my thesis defended at one of the first sessions of the Scientific Council of LNPI.

Twelve years later, O.P. Smirnov in his thesis has explained a discrepancy of our experimental data with those obtained by a computer simulation [8] of the site percolation by weak interactions between magnetic atoms in the same sublattice.

2. ***Antiferromagnetic ordering, spin dynamics and covalent spin density in the garnets with the only magnetic sublattice. A quantum effect of the zero-point spin fluctuations***

Starting from the first publication [5] we were interested in the magnetic ordering in the garnets with the only magnetic sublattice. When magnetic ions occupy either octahedral or tetrahedral sublattice there is no conventional superexchange interaction via an intermediate O^{2-}. A pair of the successively arranged two oxygen ions provides the strongest interaction. The interaction strength depends on the bond configuration, and is not necessarily stronger between the atoms with a shorter distance. As a result a variety of magnetic structures is observed in isomorphic materials with slightly different crystal structure parameters. A review of magnetic structures in the antiferromagnetic garnets, which were studied mainly in our laboratory and then were used for development of the symmetry analysis procedure, one can find in Ref. [8]. Three magnetic structures are shown in Fig. 1 for the garnets with Fe^{3+} ions in tetrahedral sublattice [9]. They differ only by non-magnetic ions in the 24c and 16a sites. Nevertheless the Néel temperature varies from 67 K for $Na_3Te_2Fe_3O_{12}$ (a) to 7 K for $YCa_2Zr_2Fe_{2.75}Ga_{0.25}O_{12}$ (c) due to a very weak difference of the atomic positions resulting in the strength of the superexchage bonds.

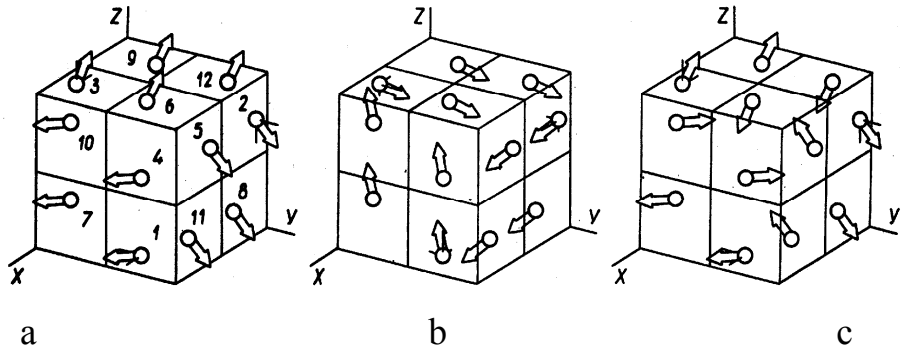

Fig. 1. Spin structures in the 24*d* sublattice of the garnets:
a – $Na_3Te_2Fe_3O_{12}$; b – $NaCa_2Sb_2Fe_3O_{12}$ and $Ca_3SbSnFe_3O_{12}$; c – $YCa_2Zr_2Fe_{2.75}Ga_{0.25}O_{12}$

Two magnetic structures (Fig. 2) have been observed for the garnets with 3*d* ions in the octahedral 16*a* sites, which form two subsystems displaced by a translation of (1/4 1/4 1/4). The Fe^{3+} spins $S = 5/2$ (a) in each subsystem of $Ca_3Fe_2Ge_3O_{12}$ (FeGeG) [10] and $Ca_3Fe_2Si_3O_{12}$ (FeSiG) [11] are ordered antiferromagnetically while Cr^{3+} spins $S = 3/2$ (b) in each subsystem of $Ca_3Cr_2Ge_3O_{12}$ (CrGeG) are ordered ferromagnetically [12]. The AFMR data show that the easy axis in both iron garnets is [111] [13], while in the chromium garnet – an axis of the [100] type [14]. (Spin ordering in the antiferromagnetic garnets was a subject of I.V. Golosovsky's thesis.) All the double-oxygen superexchange bonds are characterized by three parameters: for the nearest neighbours along a threefold axis, J_1, in the perpendicular plane, J_1', and for the next-nearest neighbours, J_2 (Fig. 2). Their values have been determined from the best fit of the spin-wave frequencies measured by inelastic neutron scattering [15, 16] as shown in Fig. 3.

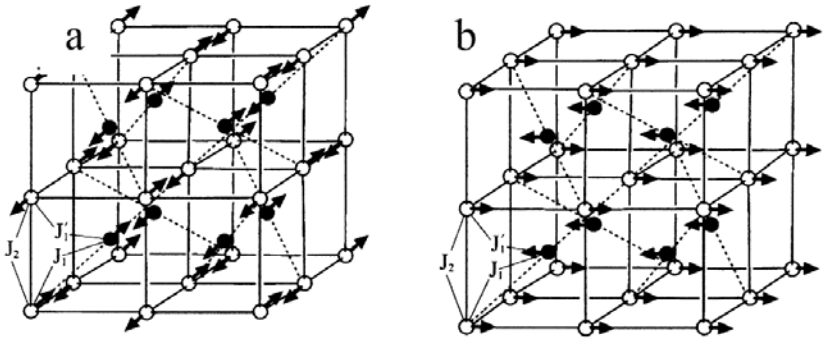

Fig. 2. Ordering of the Fe^{3+} spins (a) and Cr^{3+} spins (b) in the 16*a* sites: two subsystems (open and full circles) displaced by a translation (1/4 1/4 1/4). The dashed lines indicate the three-fold axis in each octet

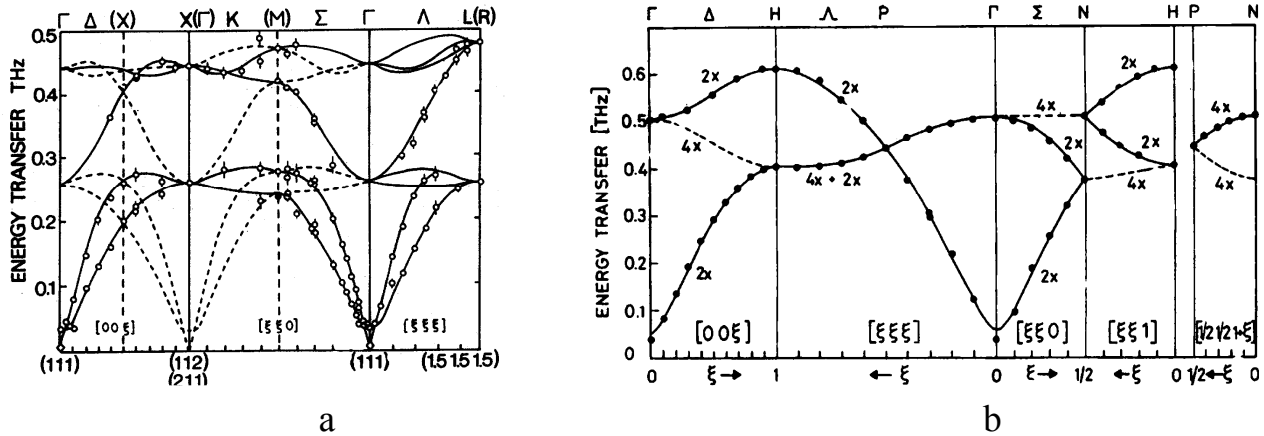

Fig. 3. Measured spin-wave frequencies (circles) and calculated dispersion curves for $Ca_3Fe_2Ge_3O_{12}$ (a) and $Ca_3Cr_2Ge_3O_{12}$ (b)

An excellent agreement of the spin-wave frequencies with the dispersion curves calculated with three variable exchange parameters plus phenomenological anisotropy parameter evidences that only the double-oxygen superexchange bonds are important. All the exchange paths, which include more than two successive oxygen atoms are much weaker. The results of refinement,

$J_1 = -0.909(9)$ K, $J_1' = -0.307(8)$ K, $J_2 = -0.615$ K for the FeGeG and

$\langle J_1 \rangle = (J_1 + 3J_1')/4 = -0.528$ K, $J_2 = 0.416$ K for the CrGeG,

are quite unusual in comparison with a conventional single-oxygen superexchange. The next-nearest-neighbour interaction is negative for the FeGeG and positive for the CrGeG, which has been explained by the different overlap between the oxygen orbitals [16]. In the case of the FeGeG the parameters J_1 and J_1' for the nearest neighbours differ by a factor of three and, which is even more unusual, the interaction J_2 for the next-nearest neighbours is two times stronger than J_1'. These unusual exchange parameters are due to the features of the double-oxygen bonds. As seen from Fig. 4, the Fe1 and Fe3 ions, the nearest neighbours along the threefold axis, are connected by three oxygen pairs, while only two oxygen pairs with longer interatomic distances connect Fe3 and Fe2 in the perpendicular plane. The overlap of these oxygen orbitals is much weaker than that between O12 and O21, which provides interaction J_2 between the next-nearest neighbours: Fe1 and Fe2 [17].

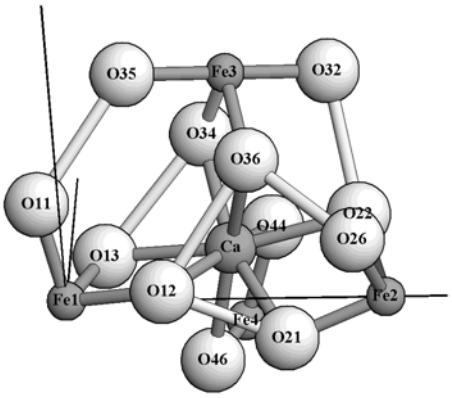

Fig. 4. A fragment of the garnet structure with four Fe^{3+} ions in the octahedral sites connected by the double-oxygen superexchange bonds. A Ca^{2+} ion is in the center.

The exchange parameters are also very sensitive to the covalent spin density transferred from a magnetic ion to the ligand. In the garnets under consideration this spin density is not cancelled as in the case of conventional superexchange via one oxygen ion [18]. To obtain this covalent moment transfer we have measured [19] the moment induced by the magnetic field, strong enough to turn the antiferromagnetic sublattices perpendicular to the field. As the field induced ferromagnetic component is equal to $m(H) = \chi H$ and reaches the ligand moment value, m_O, when the antiferromagnetic sublattices become parallel to **H** with H equal to the spin-flip field H_E, then $m_O = m(H)H_E/H$. The flipping ratio measurements provide the experimental data used in the magnetic moment calculations and in the spin density reconstruction by the maximum entropy method (MEM) as shown in Fig. 5 for the FeGeG. The least squares refinement on the basis of 183 flipping ratios, of which a set of 16 independent reflections has a purely oxygen contamination, results in $m_O = 0.12(2)\ \mu_B$ with the spin-flip field $H_E = 40.4$ T [20]. For the garnet FeSiG the same procedure results in $m_O = 0.22(3)\ \mu_B$ which correlates with the stronger interactions $J_1 = -1.16(4)$ K, $J_1' = -0.96(4)$ K, $J_2 = -1.24(4)$ K.

In the case of FeGeG and FeSiG the spins in each subsystem are ordered antiferromagnetically. From the symmetry reasons it follows that the effective field created by one subsystem at the atoms of the other one cancels out in the static molecular field approximation. The subsystems are magnetically decoupled, and the ground state is infinitely degenerated with respect to the relative orientation of the spin subsystems. The interaction should develop itself only dynamically. At one of the workshops in Zarechny during a non-official evening party, I have asked E.F. Shender, who was doing similar things, to think on this dynamical interaction. The idea of Shender [21] was very simple. In dynamics, there is an exchange interaction between transverse spin components: one, if the spins of different subsystems are orthogonal, and two, if they are collinear. As far as interaction is antiferromagnetic, a collinear configuration should be stabilized by the quantum zero-point spin fluctuations. This interaction results in an effective exchange anisotropy and as a consequence in the spin-wave gap [21]:

$$\omega_Q = -0.49(2J_1 + 6J_1')S^{1/2}. \qquad (1)$$

Using the exchange parameters given above one obtains ω_Q = 0.05 THz. This quantum exchange gap has been observed in the spin wave spectrum in our experiment [15] and is definitely seen in Fig. 3a at q = 0. Its value of 0.033(4) THz is in reasonable agreement with the calculated value and is much higher than the gap of 0.007 THz (Fig. 3a) due to the ordinary anisotropy in this garnet.

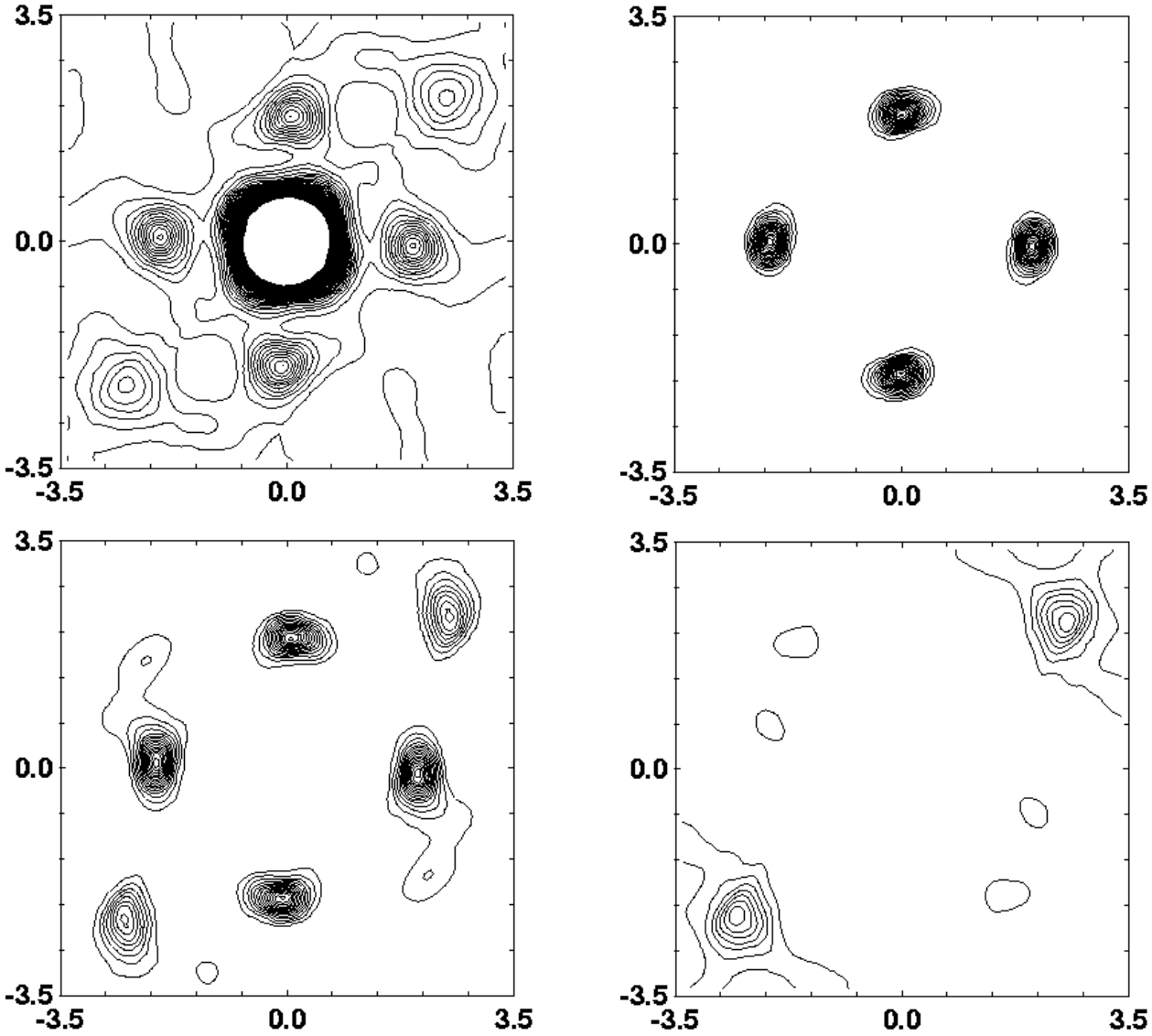

Fig. 5. Section of the three-dimensional spin density through the Fe^{3+} ion and four (of six) O^{2-} ligands as reconstructed by MEM using:
a) the complete data set of flipping ratios measured at 2 K (64 unique reflections); b) 16 unique reflections affected only by oxygen; c) all reflections except those with Fe^{3+} contribution; d) the 46 reflections contaminated by the 24*c* sites after subtraction of the calculated magnetic structure amplitude of oxygen. Density isocontours are at 0.002 $\mu_B/Å^3$ interval. Contours at the Fe^{3+} site are limited to 0.1 $\mu_B/Å^3$ for the sake of clarity. Coordinates along the axes are given in Å

3. *Weak antiferromagnetism*

The main term in the magnetic Hamiltonian is an electrostatic in nature isotropic exchange interaction

$$H_{\mathrm{H}} = \frac{1}{2}\sum_{ij} J_{ij}\mathbf{S}_i\mathbf{S}_j\,, \tag{2}$$

where J_{ij} are the exchange integrals. This Heisenberg term is symmetric to the change $\mathbf{S}_i$ for $\mathbf{S}_j$ and results in their antiparallel orientation, if $J_{ij} < 0$. Among weak relativistic interactions, which modify a collinear antiferromagnetic structure, the most important is interaction

$$H_{\mathrm{D}} = \mathbf{D}_{ij}[\mathbf{S}_i \times \mathbf{S}_j] \tag{3}$$

that had been considered phenomenologically by Dzyaloshinsky [22] and had been explained microscopically by Moriya [23]. It is seen that Dzyaloshinsky-Moriya (D-M) interaction is antisymmetric to the change $\mathbf{S}_i$ for $\mathbf{S}_j$ and stabilizes their orthogonal configuration. Microscopically this is an exchange interaction between a magnetic ion in the ground state with the other one excited by the spin-orbit coupling. H_{D} is very sensitive to the crystal symmetry. For instance, it vanishes, if there is an inversion. D-M interaction results in the ferromagnetic or antiferromagnetic spin canting. This canting is of the order of $\Delta g/g \sim 10^{-2}$, where Δg is a deviation of the g-factor from its spin value $g = 2$. Weak ferromagnetic moment due to H_{D} can be easily observed and is well studied [24]. Weak antiferromagnetism results in additional magnetic reflections with the intensity of the order of $10^{-3} \div 10^{-4}$ in comparison with the intensity due to the main antiferromagnetic component. Observation of these extremely weak reflections is very complicated since the spurious effects like higher harmonics or multiple Bragg scattering can be $1 \div 2$ orders of magnitude stronger. Nevertheless by measuring their intensity one can study anisotropic magnetic interactions, which cannot be investigated by any other method. It had been claimed that weak antiferromagnetism was observed for the first time in $CuCl_2{\cdot}2D_2O$ [25], but we had shown that this was a spurious effect.

For the first time the weak antiferromagnetism had been definitely observed in our laboratory in the yttrium orthoferrite $YFeO_3$ [26]. The orthoferrite unit cell contains 4 ions Fe^{3+} ($S = 5/2$) and 4 ions Y^{3+} or R^{3+}. (We studied the materials with R = Er, Yb.) The magnetic structure is expressed through the basis functions of the Fe^{3+}:

$$\begin{aligned}
\mathbf{F} &= (\mathbf{S}_1 + \mathbf{S}_2 + \mathbf{S}_3 + \mathbf{S}_4)/2,\\
\mathbf{G} &= (\mathbf{S}_1 - \mathbf{S}_2 + \mathbf{S}_3 - \mathbf{S}_4)/2,\\
\mathbf{A} &= (\mathbf{S}_1 - \mathbf{S}_2 - \mathbf{S}_3 + \mathbf{S}_4)/2,\\
\mathbf{C} &= (\mathbf{S}_1 + \mathbf{S}_2 - \mathbf{S}_3 - \mathbf{S}_4)/2.
\end{aligned} \tag{4}$$

Similar combinations **f**, **g**, **a**, **c** of $\mathbf{s}_1$, $\mathbf{s}_2$, $\mathbf{s}_3$, $\mathbf{s}_4$ express the polarisation of the rare earth in the field of the iron sublattice. At high temperature, when polarisation of the rare earth is weak, all the orthoferrites have magnetic structure described by irreducible representation $\Gamma_4(G_x, A_y, F_z; f_z)$. The main spin component of the Fe^{3+} is ordered antiferromagnetically along the **x**-axis like G_x. The D-M interaction leads to the weak ferromagnetic component F_z and to the weak antiferromagnetic component A_y. Every basis vector results in a series of the Bragg reflections with its own extinction law. For instance the (2 0 1) reflection is completely due to the weak antiferromagnetic component A_y. To avoid spurious effects due to the double Bagg reflections, we used the polarisation analysis technique. We had no experience in polarised neutrons, and a long stay of J. Schweizer in our laboratory was very important for our education, for performing this experiment and for development of the polarisation analysis neutron diffraction.

In Fig. 6 a Ψ-scan around the (2 0 1) scattering vector is shown. In the absence of the double Bragg scattering, the peak intensity should not depend on the Ψ. Nevertheless in the non-spin-flip mode one can see a huge intensity variation. The ω-scans are shown in Fig. 7. A strong contamination to the integrated intensity from the nearest double Bragg reflections is seen when the (201) is measured in the non-spin-flip mode, while for the spin-flip mode the double Bragg scattering is strongly suppressed, and gives no contamination to the (201). To make correction for the higher harmonics this reflection was also measured with the filter of Sm_2O_3 (Fig. 7B). As a result of this experiment the ratio of $A_y/G_x = 1.93(18)\cdot10^{-2}$ was obtained. The weak antiferromagnetic component was also found for the $YbFeO_3$ as $A_y/G_x = 1.67(6)\cdot10^{-2}$. Together with the

known value of F_z/G_x this has allowed to obtain all the components of two non-equivalent Dzyaloshinsky vectors $\mathbf{D}_1$ and $\mathbf{D}_2$ for $YbFeO_3$ as

$D_{1x} = 1.56(7), D_{1y} = 3.70(16), D_{1z} = 0, D_1 = 4.02(16)$ and
$D_{2x} = 0, D_{2y} = 1.89(8), D_{2z} = 2.76(12), D_2 = 3.34(12)$

in the units of $J_1 \cdot 10^{-2}$, where the exchange parameter $J_1 = -29.1(6)$ as obtained from the spin-wave dispersion [29].

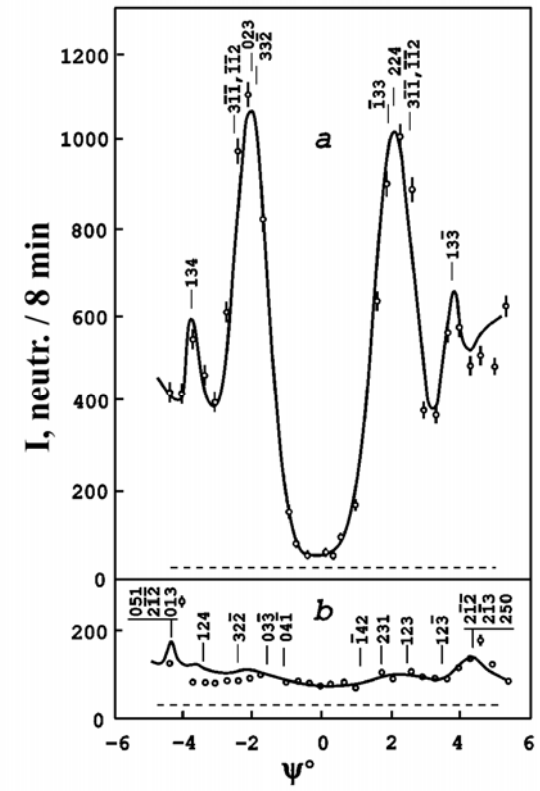

Fig. 6. Intensity variation in the peak of reflection (201) when rotating the crystal of $YFeO_3$ around the scattering vector on angle Ψ: a – non-spin-flip mode and b – spin-flip mode. The curves represent the best fit. The background level is shown by the dotted line. The positions and indices of the reciprocal lattice points involved in the double Bragg scattering are shown

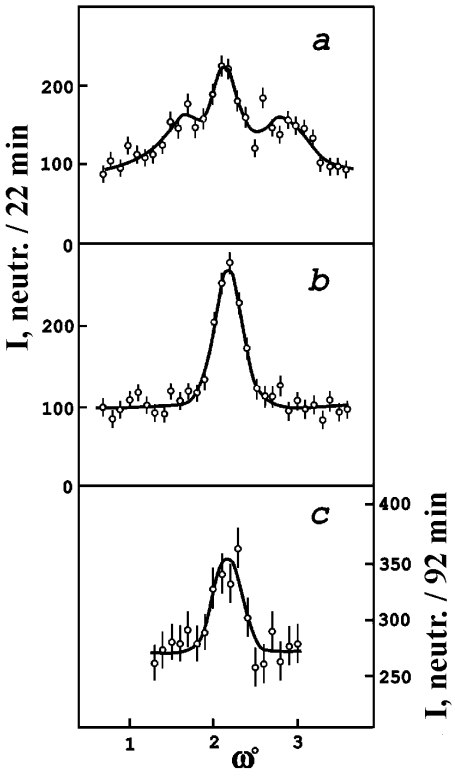

Fig. 7. The ω-scan profile of the Bragg reflection (201) $YFeO_3$ measured at $\Psi = 0$ without a filter (a, b) and with the Sm_2O_3 filter (c): A – non-spin-flip mode and b, c – spin-flip mode

In a wide temperature range below T_N the rare-earth subsystem can be considered as paramagnetic [30]. The exchange interaction is treated as Zeeman interacrion of a rare-earth ion with an effective field that is mainly produced by the antiferromagnetic component G of the Fe^{3+} spins [31]. As far as the field produced by the isotropic exchange is almost cancelled, the anisotropic R-Fe interactions become to be the most important. Unlike the Fe-Fe interactions, the anisotropic symmetric R-Fe interactions are of the same order of magnitude as the antisymmetric ones. The f_z component induced on rare earth by the iron sublattice, due to anisotropic exchange, A^{zy}_{RFe}, modifies the weak antiferromagnetic component A_y of the iron sublattice [32] as

$$A_y = -\frac{D_2^z G_x + A^{zy}_{RFe} f_z}{2J_1 - 4J_2}, \qquad (5)$$

where $J_1 = 29.1(6)$ K and $J_2 = -1.9(2)$ K [29].

The dependence $A_y(T)$ obtained from the intensity of the (001) reflection is shown in Fig. 8 for $ErFeO_3$, $YbFeO_3$ and $YFeO_3$, the latter being used as a standard with no magnetic moment in the rare-earth sublattice. The fact that the temperature dependences $A_y(T)$ and $G_x(T)$ coincide evidences that a single-ion anisotropy

contamination is negligible. This experimental curve has been used for the part of A_y non-influenced by the rare earth in $ErFeO_3$ and $YbFeO_3$ - the first term in Eq. (5). In the $ErFeO_3$, due to small polarisation of the Er^{3+} at relatively high temperatures, the effect under consideration is only around three standard deviations $A_{RFe}^{zy} = 0.032(9)$, which gives only the sign of interaction. In the case of $YbFeO_3$ the feedback of the polarised rare earth and the polarising iron sublattices clearly decreases A_y at low temperature: $A_{RFe}^{zy} = -0.20(1)$.

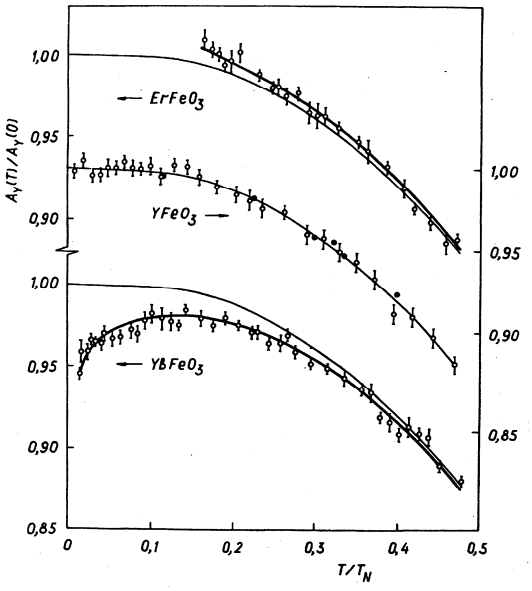

Fig. 8. Dependence $A_y(T)$ for $ErFeO_3$, $YFeO_3$ and $YbFeO_3$. Solid circles are magnetisation of the Fe^{3+} sublattice in $LaFeO_3$

The first observation of the weak antiferromagnetism in the orthoferrites and investigation of the anisotropic symmetric and antisymmetric interactions, as well as a design of the new diffractometer have made a basis for the thesis of Yu.P. Chernenkov.

Moriya [23] had predicted the weak antiferromagnetism due to the antisymmetric exchange interaction for the $CuCl_2 \cdot 2D_2O$. Experimental results [25] were obviously erroneous since the magnetic form-factor for the week antiferromagnetic component differed very much of that for the main spin component. (If the weak component is due to the D-M interaction, the spatial distribution of its spin density should be the same as for the main one.) On the other hand, if the quantization axes for the spin and the angular momentum are different, the spin-orbit coupling may result in a non-spherical component of the spin density being equal to zero when averaged over the atom [33]. The unit cell of the $CuCl_2 \cdot 2D_2O$ doubled along **z**-axis due to magnetic ordering is shown in Fig. 9.The ion Cu^{2+} is coordinated by an octahedron of four Cu^{1-} ions (1, 2, 4, 5) and two O^{2-} ions (3, 6). The axes of an octahedron ξ, η, ς are the quantization axes for the ground-state wave function $\Psi_1 = c_0\varphi_0 + 2^{-1/2} c_2 (\varphi_2 + \varphi_{-2})$, where φ_0, φ_2, φ_{-2} are the one-electron wave functions. The angle between ξ and ς is nearly 90°, η coincides with **y**, while ς is inclined to **z**-axis by the angle $\kappa = 37.5°$.

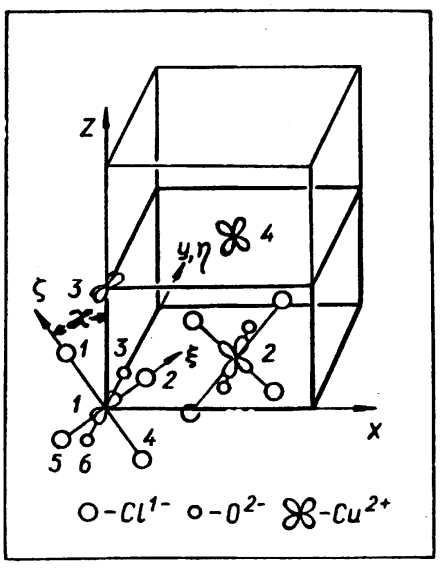

Fig. 9. The magnetic unit cell of the $CuCl_2 \cdot 2D_2O$. The coordination of two Cu^{2+} ions is shown

The ordering of the main spin component in the magnetic unit cell is described by the basis function

$$C_x = (S_{1x} + S_{2x} - S_{3x} - S_{4x})/2, \quad (6)$$

while the weak antiferromagnetic component by the

$$A_z = (S_{1z} - S_{2z} - S_{3z} + S_{4z})/2 \quad (7)$$

as shown in Fig. 10. These basis vectors result in two sets of magnetic reflections with different extinction law:

$$C_x \rightarrow (h + k = 2n, l = 2n+1); \quad (8)$$

$$A_z \rightarrow (h + k = 2n + 1, l = 2n+1). \quad (9)$$

Altogether 7 reflections of the C-type and 4 reflections of the A-type were measured in conditions, which exclude any contamination from the double Bragg scattering. (For each A-reflection the appropriate angular position was calculated.) The contamination from the second harmonics was as low as 10^{-5} [34]. The magnetic form-factor for both sets of reflections has been calculated on the basis of the ground-state wave function that takes into account spin-orbit coupling and the fact that the angular moment quantization axis is inclined [35]. The spin part of the main component

form-factor is $F_x^s(q) = 1/2$ at $q = 0$. Corresponding orbital contamination is $F_x^l(0) = -\Delta g_x / 4$, where $\Delta g_x = g_x - 2$. The form-factor spin part for the *A* reflections, $\mathbf{f}^s(\mathbf{q})$ is orthogonal to **C**. It is completely non-spherical and is equal to zero at $\mathbf{q} = 0$. Its orbital part is expressed as

$$f_z^l(0) = \tfrac{1}{8}(g_\zeta - g_\xi)\sin 2\kappa . \qquad (10)$$

It is seen that a weak antiferromagnetic component due to the angular moment appears:

$$\frac{A_z}{C_x} = \frac{g_\zeta - g_\xi}{2g_x}\sin 2\kappa . \qquad (11)$$

Using experimental data [36] for the *g*-tensor one obtains from (11) the weak antiferromagnetic component due to the unfrozen angular momentas $A_z/C_x = 0.050(2)$.

From the least-squares refinement on the set of *C*-reflections an admixture coefficient $c_0 = 0.05(4)$ and the scale factor were determined. Their values were used in the form-factor refinement for the *A*- reflections with the only variable A_z/C_x, that was obtained as $A_z/C_x = 0.062(2)$. The experimental and the calculated values of the form-factor for the main *C*-reflections (001, 021, 003, 023, 041, 043) as well as for the weak *A*-reflections are displayed in Fig. 11, where the curve represents the integral $\langle j_0 \rangle$ for the spherically symmetric part of the form-factor.

It is worthwhile to point out that the value $A_z/C_x = 0.062(2)$ includes both the orbital and D-M parts of the weak antiferromagnetic moment. Subtracting the orbital part given above one obtains for the weak antiferromagnetic component due to the D-M antisymmetric interaction only a small value of $A_z/C_x = 0.012(3)$. But this point needs an additional experiment to obtain the form-factor at higher $\sin\theta/\lambda$.

The investigations of $CuCl_2 \cdot 2D_2O$ have been used in the thesis of V.A. Galushko from the Physical-Technical Institute (Donetsk).

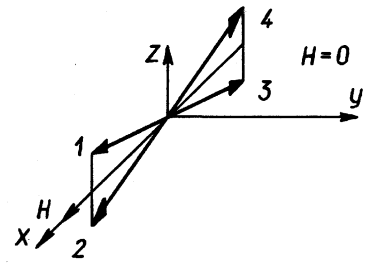

Fig. 10. Zero-field spin ordering in the $CuCl_2 \cdot 2D_2O$. The main spin components along **x** and the weak component along **z** are shown

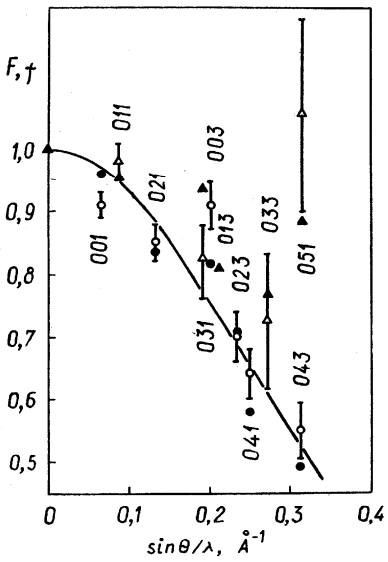

Fig. 11. The Cu^{2+}magnetic form-factor. The filled and the open circles are, respectively, theoretical and experimental values for the main C_x - component; the filled and the open triangles are the same for the weak A_z - component

4. *Magnetic ordering in ferroelectrics*

As mentioned in the preface, the first material investigated by neutron diffraction at the WWR-M reactor was the first discovered ferroelectric with antiferromagnetic ordering $BiFeO_3$ [2]. The second work in this field was an investigation of the magnetic ordering in the ferroelectrics with the perovskite structure $PbFe_{1/2}Nb_{1/2}O_3$ and $PbFe_{1/3}W_{2/3}O_3$ [37, 38]. The most important property of these materials is a spontaneous magneto-electric effect, which means an appearance of the magnetic (electric) moment simultaneously with the ferroelectric (magnetic) ordering. One of its possible microscopic mechanisms is an influence on the spin-orbit coupling of the Stark splitting of the magnetic ion levels in very high electric fields [39]. The other one is an influence of the electric field due to ferroelectric atomic displacements up to about 0.1 Å on the exchange parameters [40]. Trying to study these non-trivial mechanisms we came back to the antiferromagnetism in ferroelectrics once in a decade.

Materials with the general formula $M_3B_7O_{13}X$, where *M* is a bivalent 3*d*-ion, and *X* is a halogen, represent the next structure class studied in our laboratory. They have the structure of the mineral boracite

$Mg_3B_7O_{13}Cl$ [41] that gives the name to all the class. We have studied the structural and magnetic phase transitions in the Co-I and the Fe-I boracites [42 – 44]. An additional change of magnetic structure was observed in the Co-I boracite below the Néel temperature. The analysis of the magnetic ordering and the atomic displacements in Fe-I boracite suggests that the dipole structure that appears at the ferroelectric transition drastically decreases the superexchange interaction. These neutron and X-ray diffraction studies of the boracites were used in the thesis of A.V. Kovalev.

Another decade had passed, and we (mainly V. A. Polyakov) started to study a new class of magnetic fer-roelectrics with the general formula $R\mathrm{Mn_2O_5}$, which definitely show very strong magneto-electric coupling [45-48]. These materials in the paraelectric phase have the orthorhombic structure with the space group *Pbam*. The Mn^{3+} ($S = 2$) and Mn^{4+} ($S = 3/2$) ions occupy 4*h* and 4*f* sites in the square oxygen pyramids and in the oxygen octahedra, respectively. For the beginning we have chosen $EuMn_2O_5$ since Eu^{3+} is non-magnetic, and the low-temperature properties should be simpler than in the other isomorphic materials. Very strong and sharp peaks of the dielectric permittivity were observed for the Eu- material at $T_{C1} \approx 35 \div 40$ K and $T_{C2} \approx 21 \div 22$ K [45, 47]. They are accompanied by the anomalies of magnetic susceptibility. We have found that the magnetic ordering occurs below $T_N = 40(1)$ K with the propagation vector $\mathbf{k} = [1/2\ 0\ 0.3]$. Down to $T = 35$ K, the k_z component is changing to the commensurate value $k_z = 1/3$ that stays to the liquid helium temperature. The transition from $k_z = 0.3$ to $k_z = 1/3$ is of the first order as seen in Fig. 12a. The $k_z = 1/2$ stays stable, but at about 16 K the additional wave vectors $\mathbf{k}_{2,3} = [1/2 \pm \delta\ 0\ 1/3]$ appear with $\delta \approx 0.002$. A slight anomaly in the (1/2 0 1/3) intensity is seen at the lock-in temperature of 35 K (Fig. 12b). The (1/2 0 1/3) intensity changes drastically in the vicinity of the T_{C2} with the further hysteretic change at about 16 K.

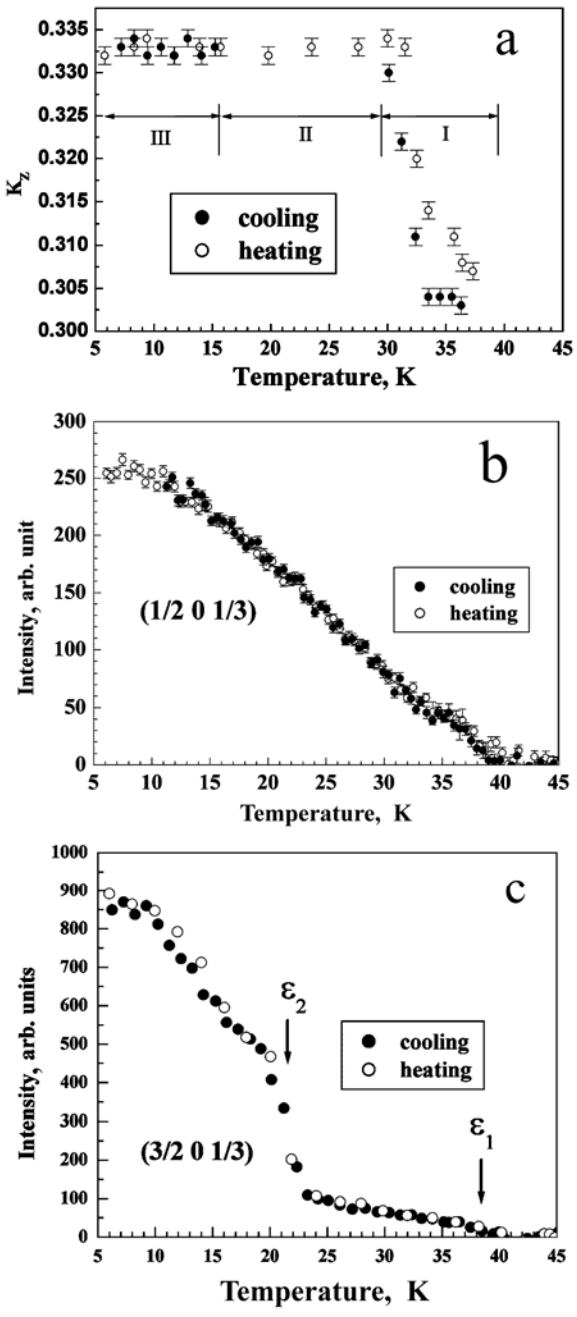

Fig. 12. The magnetic propagation vector (a) and intensity of the magnetic reflections (1/2 0 1/3) – (b), (3/2 0 1/3) (b) – (c) *vs*. temperature

The magnetic structure is not determined yet, but we have found the atomic displacements in two ferroelectric phases [49]. In all the temperature range be-low T_{C1} the Mn^{3+} ions are displaced nearly along the pyramid axis as shown in Fig. 13. Four Mn^{3+} ions are split into two pairs, and the displacements do not depend on the temperature down to $T = 6$ K: $\Delta x_1 = -0.078(2)$ Å, $\Delta x_2 = -0.057(3)$ Å. At $T = 6$ K the displacements of Mn^{4+}, $\Delta y = -0.027(2)$, and Eu^{3+}, $\Delta y = -0.046(2)$, have been found.

The most intriguing result is a modulation of the crystal structure with the wave vector of the magnetic structure that has been found at $T = 10$ K by measurements of the non-spin-flip intensity with the initial polarisation along the scattering vector. This is an actual microscopic evidence of the magneto-electric interaction. The results are preliminary, and the experiment will be continued to measure a number of non-magnetic contaminations to the magnetic reflections, which would be sufficient for the determination of atomic dis-

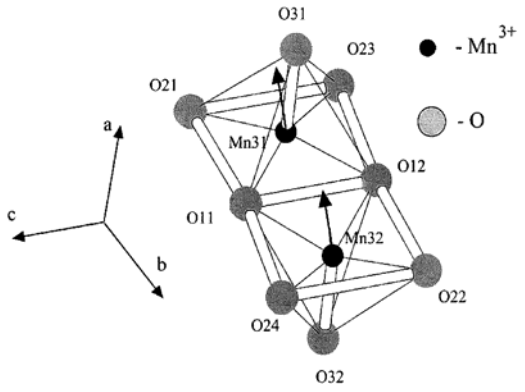

placements due to this modulation. Since 1987 we regularly use a method of polarisation analysis, which gives sometimes principally new information that cannot be obtained by the other neutron scattering methods.

Our activities on the magnetically ordered ferroelectrics show that the process of cognition is similar to a spiral. Every next pitch gives more precise knowledge than the previous one.

Fig. 13. Ferroelectric displacements of the Mn3+ ions

5. *X-ray studies of the molecular structure of proteins*

During the opening of the monument of B.P. Konstantinov near the main entrance in 1977, I had happened by chance to stay near S.E. Bresler. He was always dreaming of the protein structure investigations by the X-ray diffraction method and proposed me to participate in this program. This was actually a "long way to Tipperary". The first step was to build the X-ray laboratory starting from the construction stage on the place of a shop at the building No 50. Then we found some equipment sufficient for the preliminary studies. A complete set was too expensive, and moreover at that time it became clear that the final measurements should be normally carried out using synchrotron X-rays. The main event in our protein crystallography program had happened in 1985 with the appearance in the laboratory of A.M. Golubev. Unfortunately he spent quite long time trying to grow a crystal of RecA, a protein that takes part in the DNA recombination.

Fig. 14. Graphical representation of the structure of α–galactosidase, glycoprotein from *Trichoderma reesei* with the resolution of 1.54 Å. The molecules of a polysaccharid attached to the protein are also shown

The actual success has come with biochemical and structural studies of carbohidrases, ensymes participating in hydrolisis of polysaccharides. The first molecule studied is glucoamylase from *Aspergillus awamori*. It is a good model to investigate the postsecretory processing of glycoproteins. It has been shown that mechanism of deglycosylation of glucomylase by own α–mannosidase *in vivo* removes polysaccharide protection of the glycoprotein and causes following partial proteolysis as well as the appearing of a new, so-called minor form of the glucoamylase. Now the number of carbohydrases is increased. Various aspects of catalytic mechanisms have been explained using biochemical approaches [50, 51], and new enzymes have been crystallized [52, 53]. A fruitful collaboration has been established with Brazilian Synchrotron Centre. Thus, structure of asparic proteinase from *Trihoderma reesei* was solved. Native protein and its complex with pepstatin A – inhibitor is crystallized. Recently the structure of α–galactosidase from *Trichodema reesei* shown in Fig. 14 has been solved. It should be stressed out that only one Cs-derivative with anomalous signal (SIR method) has been used. Co-crystallisation with an inhibitor, D-galactose, has helped to localize the active site of the enzyme. The works on explanation of the catalytic mechanism of

the α–galactosidase are in progress. Certainly many of these achievements were possible owing to the permanent support from the late V.N. Fomichev and due to collaboration with a biochemical group of K.N. Neustroev from the Division of Molecular Radiation Biology.

6. *The age of the high-T_C superconductivity*

I always avoided studying something popular that everybody in the world is doing. One cannot make anything original and actually new being in a crowd. But in the case of the high-T_C superconductivity the phenomenon itself was so unusual, and the world activities were so intense that we had joined them. We used our experimental potential including polarisation analysis of scattered neutrons [54], the instrument designed mainly by A.G. Gukasov (now to Saclay, France), after the successful studies of the weak antiferromagnetism, powder neutron diffraction on the 40-detector diffractometer designed by I.V. Golosovsky and the possibilities of the X-ray single crystal scattering, which were not sufficient for the protein crystallography, but happened to be good enough for the high-T_C investigations. A.B. Stratilatov (now to Windsor University, Canada), Yu.P. Chernenkov and V.I. Fedorov did a big deal of the X-ray instrumentation. The high-T_C materials and the parent compounds were studied. Having this technique we investigated the crystal structure of the most popular system $YBa_2Cu_3O_{6+x}$ (YBCO) and the spin ordering and the spin fluctuations in two very similar classes of the high-T_C materials and their parent compounds: La_2CuO_4 and R_2CuO_4 (R = Nd, Pr, Sm, Eu, Gd) with the tetragonal structures called T and T$'$, respectively.

Historically the YBCO was the first system we had started with. There are two possible copper sites in the YBCO structure [55, 56]: in the plains CuO_2 with two copper atoms per the unit cell, Cu(1) – (0,0,0) in the plane z = 0, in which the oxygen content can be changed in the limits $0 \le x \le 1$ and Cu(2) – (0,0,±z). Each Cu(1) ion is coordinated by two apical oxygen ions O(1) – (0,0,±z). At x =0, the Cu(1) has no other oxygen neighbours in the basal plane and, being twofold coordinated, is monovalent. This material has tetragonal structure with the equivalent oxygen ions O(2) – (1/2,0,±z) and O(3) – (0,1/2,±z) in the CuO_2 plane. It is an insulator with the antiferromagnetic ordering of the Cu^{2+} spins in the CuO_2 planes. The neutral oxygen incorporated in the basal planes takes two electrons from the nearest Cu^{1+} ions forming the Cu–O chain fragments [57], the length of which grows with the increase of x, and at $x \approx 0.4$ the structure becomes orthorhombic with the additional O(4) – (0,1/2,0) in the chain. Simultaneously the superconductivity appears. The T_C jumps from 0 K to about 60 K, stays stable to $x \approx 0.6$ and then increases to the highest value of $T_C \approx 91 \div 95$ K at $x \ge 0.93$. The oxygen ordering into –O–Cu–O– chains induces carrier doping of the CuO_2 layers with increasing x, which give rise to superconductivity.

It was observed [58] that treatment of non-superconducting YBCO with $x \approx 0$ by the chlorine gas makes the material to be superconducting with $T_C \approx 90$ K. Using joint many-phase profile analysis of the data obtained by the powder neutron and X-ray diffraction we have understood the mechanism of this phenome-non. The Cl^{1-} enters the CuO_2 planes leaving the original unit cell to be tetragonal. The oxygen substituted by chlorine enters the oxygen-deficient CuO planes, but in another grains making them to be superconducting, with the amount of oxygen corresponding to the $T_C \approx 90$ K [59]. A joint profile analysis of the neutron and the X-ray data has been made for the first time. This allows finding the concentration of two different ions in a given site. Taking into account a coexistence of two phases together with some amount of an amorphous material this was a very hard job. Moreover, the M4030 computer used in this analysis took around half an hour for one least-squares cycle while an average time between rebooting the computer was 20 minutes. Now it seems unbelievable that together with E.I. Fedorova we have spent half a year to obtain these results.

Our main activity on YBCO was the structure studies connected with the oxygen ordering in the basal plane. The oxygen-rich and oxygen-poor chains along the [010] direction ord+er in the [100] direction. By the X-ray scattering we have found [60] that in the range $0.40(3) \le x \le 0.63(3)$ each oxygen chain alternates with a vacant one (ortho-II phase). The crystals with $0.70(3) \le x \le 0.80(3)$ possess another superstructure [61] with alternating two oxygen and one vacant chains, which triples the unit cell (ortho-III phase). This ordering is of the short-range type with different correlation lengths, $\xi_y >> \xi_x >> \xi_z$. A method of profile analysis of the single crystal diffuse scattering due to the short-range order has been developed [60], and the atomic dis-

placements shown by arrows in Fig. 15 are determined in both phases by the joint least-squares refinement on the X-ray and the neutron scattering data [60-64]. It is worthwhile to mention that the neutron data have become available only with a big single crystal of about 40 mm^3 grown by J.Y. Henry. This is why all the neutron data were obtained at the SILOË reactor at CENG (France). The atomic displacements due to the oxygen ordering, although small, change significantly the interpretation of many experimental results that have been treated on the basis of the average structure. This is the case for the experiments concerning the crystalline electric field (CEF) on the rare-earth ions that occupy the position of yttrium and according to our data should be displaced along **x** about 0.01 Å. The intrinsic CEF parameters B_n depend on the distance to the ligands as $(R/R_0)^{t_n}$, where R_0 is the mean distance, $t_4 = 9.9$ and $t_6 = 3.9$. The parameters B_4 and B_6 can vary as much as 4.2% and 1.6%, respectively, which is of the order of magnitude as observed in experiment and explained by the charge transfer. The YBCO results have been used in the thesis of A.B. Stratilatov.

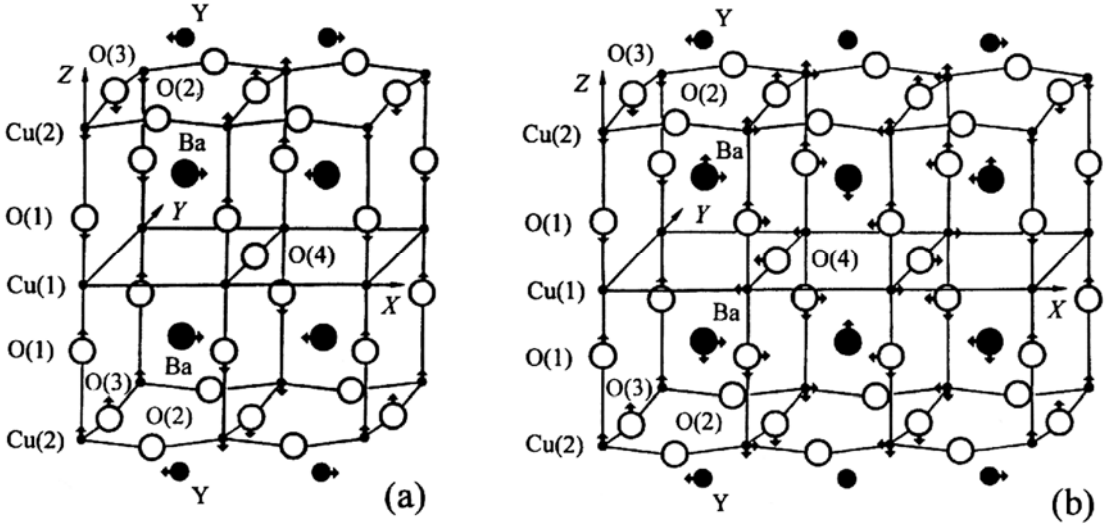

Fig. 15. The structures of the ortho-II (a) and the ortho-III phases

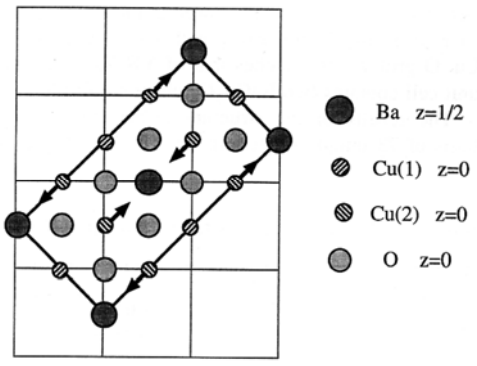

Fig. 16. The structure of $BaCu_3O_4$. The square grid is that of the CuO_2 layers of YBCO

A lattice gas (so-called ASYNNI) model [65] gives very simple explanation of the linear ordering of the –O–Cu–O– chains studied in our experiments [60-64]. It is based on the assumption that there is a repulsion between the nearest oxygen atoms in a corner configuration and a strong attraction in a linear configuration due to the hybridisation of the oxygen *p*-orbitals with the $d_{z^2-y^2}$ or $d_{z^2-x^2}$ of an intermediate Cu(1). However, the herringbone-like superstructure with the unit cell $2\sqrt{2}a_0 \times 2\sqrt{2}a_0 \times c_0$ was observed by the electron [66] and the neutron [67] diffraction. This superstructure is in the evident contradiction with the ASYNNI model, and possesses an important test of the above theory. This is why we have tried to confirm its existence. On the contrary, we have found that the additional reflections observed in Refs. [66, 67] are due to an alien phase [68]. On the basis of 341 reflections measured with synchrotron X-rays, it is shown that neither oxygen ordering in a herring-bone-like scheme nor any other superstructure in the YBCO lattice can explain the diffraction pattern. This phase, representing less than 0.2% of the whole sample volume, corresponds to an intergrowth by epitaxy upon the CuO_2 layers of YBCO. The chemical formula is determined as Ba_3CuO_4 [69]. The structure of this compound with the orthorhombic space group *Cmmm* and the lattice parameters a = 10.94(2) Å, b = 5.47(1) Å, c = 3.91(1) Å is characterized by a stacking of Cu_3O_4 layers connected by

barium atoms. It is described in Fig. 16. The flat cop-per-oxygen layers contain ordered vacancies on the copper sites with two vacancies per unit cell. The Cu atoms are displaced by 0.028(4) Å towards the vacancies as shown by the arrows. These re-sults together with the oxygen treatment of the YBCO crystals in the ortho-II phase have entered the thesis of F. Yakhou, a thesis student in the Fourier University of Grenoble.

One of the most promising mechanisms considered for high-T_C superconductivity was electron coupling connected with magnetism. The first high-T_C superconductors were obtained in the layer cuprates by doping, which introduced the charge carriers (normally the holes). The parent compounds are antiferromagnetic insulators with very high superexchange interaction of about 1000 K between the Cu^{2+} ions (S = 1/2) that provides the Néel temperature of $T_N \approx 300$ K. (Actually, because of the very strong covalency and the quantum zero-point fluctuations the Cu^{2+} moment in all these compounds is found to be roughly a half of the expected value of about 1 μ_B.) In the first high-T_C material $La_{2-x}Sr_xCuO_4$, the T_N falls down to zero at $x \approx 0.04$, and in the range of the Sr^{2+} concentration of about 0.08 ÷ 0.22 the superconductivity exists with the maximal $T_C \approx 40$ K. Two dimensional spin fluctuations have been observed in the magnetically ordered phase above T_N. They also exist in the superconducting phase, but with the correlation length decreasing as $\xi(x) = 3.8x^{-1/2}$ Å [70], which makes them hardly observable. To measure the scattering on these two-dimensional fluctuations, which are quasielastic, one has to integrate over the energy transfer along the magnetic rods [001] in the reciprocal space. Such a focusing scan [h, 0, 0.625] is shown in Fig. 17. A purely magnetic intensity, I_m is displayed. It was obtained from the spin-flip (*SF*) and non-spin-flip (*NSF*) intensities with the initial polarisation along (x), across (y) the average scattering vector and perpendicular to the scattering plane as

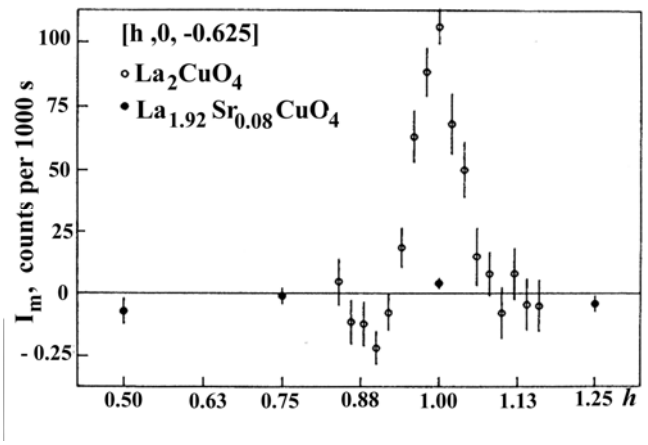

Fig. 17. Purely magnetic scattering on the two-dimensional spin fluctuations in La_2CuO_4 and in $La_{1.92}Sr_{0.08}CuO_4$ at room temperature and at T = 4.2 K, respectively

$$I_m = I_x^{SF} + I_y^{SF} - 2I_z^{SF} = -I_x^{NSF} - I_y^{NSF} + 2I_z^{NSF} \quad . \tag{12}$$

The relative values of I_x, I_y, I_z indicate that the2D spin fluctuations in La_2CuO_4 are isotropic [71], and the width of the peak in Fig. 17 gives their correlation length as ζ = 75(15) Å. The peak intensity for $La_{1.92}Sr_{0.08}CuO_4$ is equal to zero in the limits of the standard deviation, and is estimated to be about 50 times weaker than that for La_2CuO_4. According to [70] it should be only about 8 times weaker, and we suppose that the discrepancy is due to the gap, like in $YBa_2Cu_3O_{6+x}$ [71], and a restricted range of the energy integration in our case.

The magnetic phase transitions have been studied in Nd_2CuO_4, which becomes a superconductor with the electron carrier when doped by Ce. The structure of this material (so-called T') differs from that of La_2CuO_4 (T-structure). In the latter the Cu^{2+} ions are coordinated by the oxygen octahedra while in the former they are fourfold coordinated by the oxygen ions. Using the polarisation analysis method, the magnetic ordering in three phases of Nd_2CuO_4 and in the cerium-doped Nd-cuprate has been determined as well as in the isomorphous cuprates of Pr, Eu [72], Gd [73] and Sm [74]. Two types of the Cu^{2+} spin ordering have been found. Measuring of six components, I_x^{SF}, I_y^{SF}, $2I_z^{SF}$, I_x^{NSF}, I_y^{NSF}, $2I_z^{NSF}$, offers a possibility to find the spin structure from a restricted number (usually two) of magnetic reflections. The ordering of the rare-earth moments at low temperature has been also determined. Because of high neutron absorption of the natural Gd, Eu, Sm, their low-absorbing isotopes were used. As a result practically all the T'-series have been studied in our laboratory, mainly by I.A. Zobkalo, and is included in his thesis together with the $La_{2-x}Sr_xCuO_4$ system.

Magnetic properties of the quantum antiferromagnets R_2CuO_4 with the T'-structure are very interesting by themselves, and their neutron scattering studies appear to be important independently on the possible mechanisms of the high-T_C superconductivity. Very strong in-plane exchange interaction stabilizes a collinear anti-ferromagnetic ordering with the wave vector (π/a)[1, 1, 0]. Due to the body centring, the molecular fields from one CuO_2 layer on each copper atom in the adjacent ones and vice versa are cancelled. In this situation the mutual spin orientation should depend on some weak interactions. The diffraction experiments [75, 76] performed in the external field applied along the [1, 1, 0]-type direction give evidence that the Cu^{2+} spins in adjacent layers are orthogonal, like in the Pr cuprate and in the phases I, III of the Nd one (Fig. 18a) or in the Eu, Sm cuprates and in the phase II of the Nd one (Fig. 18b). These orthogonal spin structures are shown [77] to be stabilised by the pseudodipolar interaction:

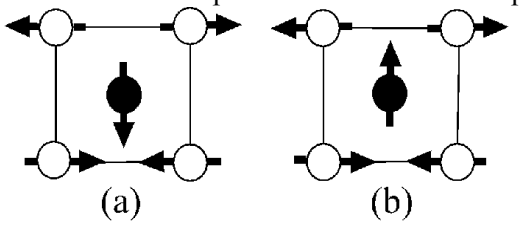

Fig. 18. Two types of the Cu^{2+} spin ordering in R_2CuO_4: (a) R = Nd in the phases I, III and Pr; (b) R = Nd in the phase II, Eu and Sm. Open and closed circles represent the Cu^{2+} ions at $z = 0$ and $z = 1/2$, respectively

$$\Delta E_{PD} = Q \sin(\varphi_1 + \varphi_2) \qquad (13)$$

and by the intraplane square anisotropy. Here φ_1 and φ_2 determine the orientations of the corner and central spins. At $H = 0$, the structures (a) and (b) correspond to $Q < 0$ and $Q > 0$.

The spin-flop transition at $\mathbf{H} \| [1,1,0]$ is of the second order [76], and at low temperature the subsystems are rotated by the angles φ and $-\varphi$ determined as [77]

$$\sin 2\varphi = (g\mu H/\Delta_0)^2 \qquad (14)$$

where Δ_0 is the in-plane spin-wave gap at $H = 0$.The angle $\alpha = \pi/4 - \varphi$ depends on the reduced field $h = (H_c - H)/ H_c$ as $\alpha \propto h^{1/2}$ at small h. But at $h << 1$ $\alpha \propto h^{1/4}$ due to interaction between the field component parallel to the sublattice magnetisation and the turned transverse spin components, which is equivalent to $\Delta_0 \to 0$ [77], or to Bose-Einstein condensation of the magnon Bose-gas [78]. The magnetic Bragg intensity, I_M, is proportional to $\sin^2\alpha$. This means that in the vicinity of the spin-flop transition a cross-over from $I_M \propto h$ to $I_M \propto h^{1/2}$ should occur. This crossover has been actually observed in Pr_2CuO_4 at $T = 4.5$ K as shown in Fig. 19.

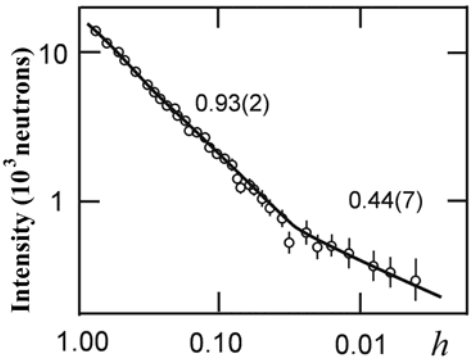

Fig. 19. A log-log plot of the intensity of the magnetic peak (1/2, 1/2, 1) *vs.* reduced field h

7. *Spin chirality*

A spiral organization of matter is widespread. The spiral structure is typical for the biological molecules, like DNA and proteins. A protein, like α–galactosidase, shown in Fig. 14 consists of the amino-aside chain, partially screwed in so-called α–spiral. The spiral screw is characterised by chirality - the direction of rotation when going along the spiral. All the natural proteins have the same, right-handed, chirality as seen in Fig. 14. The artificial polypeptide chains are equally the right- and left-handed. The simplest chiral systems, in which the chirality can be studied quantitatively, are widely presented among the magnetic materials. Two examples are shown in Fig. 20. The frustration of the nearest –neighbour spins in a triangular lattice antiferromagnets like $CsMnBr_3$ is resolved by their 120º ordering. In the rare-earth metals like Ho, due to the long-range oscillating interaction RKKY, the spins in each plane (001) are ordered ferromagnetically, but turn when propagating along **z**-axis. In both cases the order parameter includes, along with the ordinary spin variable $\mathbf{S_R}$, the spin chirality

$$\mathbf{C} = [\mathbf{S_{R1}} \times \mathbf{S_{R2}}] \, . \qquad (15)$$

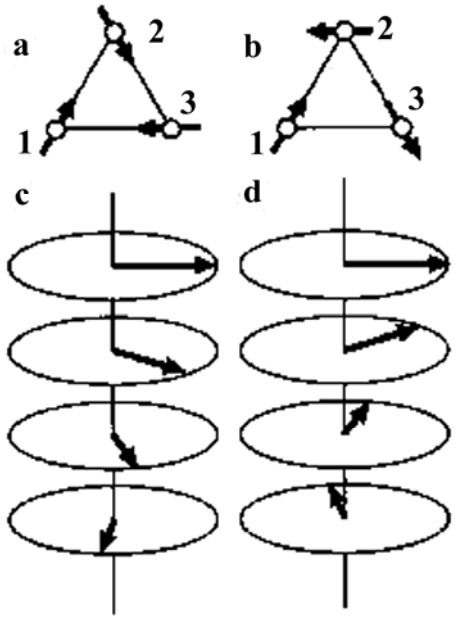

Fig. 20. Right- and left-handed chiral domains in a TLA like $CsMnBr_3$ (a), (b) and in a simple spiral structure like holmium (c), (d).

This is a relevant two-point variable that describes the clock-wise or anti-clockwise rotation between the nearest in-phase planes containing $\mathbf{S_{R1}}$, $\mathbf{S_{R2}}$ and perpendicular to the wave vector $\mathbf{k}$ of the magnetic structure. For $CsMnBr_3$ $\mathbf{k} = \frac{1}{3}(\mathbf{b}_1 + \mathbf{b}_2)$, and for Ho $\mathbf{k} = \mu\mathbf{b}_3$, where $\mathbf{b}_1$, $\mathbf{b}_2$, $\mathbf{b}_3$ are the reciprocal lattice vectors.

A twofold additional degeneracy (Z_2) changes the $SO(2)$ symmetry of an XY magnet, two types of which were mentioned above to $Z_2 \times SO(2)$. If the antisymmetric Dzyaloshinsky-Moriya exchange interaction (3) is forbidden as in the centro-symmetric crystals, there is no other known purely solid-state interaction to remove the degeneracy of the right- and the left-screw helical states, and they are realized in separate domains with equal probabilities (populations) $n_R = n_L = 1/2$. As it has been shown by Zhizhimov and Khriplovich [79], the parity violation in the framework of the standard model of weak interactions results in the P-odd long-range interaction between magnetic ions via the conducting electrons, which lowers the energy of the left-screw helix in Ho by about 100 Hz resulting in a small $(n_R - n_L)$, if any difference due to the crystalline growth is equal to zero. The $(n_R - n_L)$ can be obtained from the polarisation-dependent (PD) part of the magnetic satellite intensity [80] that is given by the second term in Eq. (16):

$$I(\mathbf{Q}) \propto f^2(\mathbf{Q})\{\langle S_z\rangle^2[1+(\hat{\mathbf{Q}}\hat{\mathbf{C}})^2] + 2\langle C\rangle(\hat{\mathbf{Q}}\hat{\mathbf{C}})(\hat{\mathbf{Q}}\mathbf{P}_0)(n_R - n_L)\}\delta(\mathbf{Q}-\mathbf{b}-\mathbf{k}), \qquad (16)$$

where the scattering vector $\hat{\mathbf{Q}}$ is a unit vector along the transferred momentum $\mathbf{Q}$, $\hat{\mathbf{C}}$ is a unit vector along $\mathbf{C}$ (either [001] or $[00\bar{1}]$), $\mathbf{P}_0$ is the initial polarisation, The δ-function reflects the Bragg condition , $\mathbf{Q} = \mathbf{b} + \mathbf{k}$, for a magnetic reflection with the wave vector $\mathbf{k}$. In order to determine $(n_R - n_L)$, one has to measure the difference $\Delta I = I^{\uparrow} - I^{\downarrow}$ with $\mathbf{P}_0$ parallel and antiparallel to $\mathbf{Q}$.

We found the difference $(n_R - n_L) \sim 10^{-3}$ in the samples that were prepared of the filings filed off from the polycrystalline ingot, with the sign that depended on the file direction, along or across its movement. No asymmetry at the level of 10^{-5} was found in the samples without a memory of mechanical treatment. Therefore, instead of the parity violation we have found the interaction of chirality with the torsion deformation [81]. In Ref. [82] a single crystal of holmium with the difference $(n_R - n_L) \sim 5\cdot 10^{-2}$ has been prepared by the torsion around $\mathbf{C} \| [001]$. Apparently the simplest expression for this interaction [81] should have the form:

$$W = \sum_{\mathbf{R}1,\mathbf{R}2} g(\mathbf{R}_{12})[\mathbf{S}_{\mathbf{R}1} \times \mathbf{S}_{\mathbf{R}2}] \cdot (\mathrm{rot}\mathbf{u}_{\mathbf{R}1} - \mathrm{rot}\mathbf{u}_{\mathbf{R}2}), \qquad (17)$$

where $\mathbf{u_R}$ is the displacement of the atom in a lattice point $\mathbf{R}$ from its equilibrium position, and the energy $g(\mathbf{R}_{12})$ determines the strength of interaction.

The chiral antiferromagnets have attracted considerable interest because of Kawamura's conjecture (see [83] and references therein) that their spin-order transitions should belong to new chiral-universality classes characterized by the modified critical exponents α for the specific heat, β for the staggered magnetization, γ for the susceptibility and ν for the inverse correlation length, together with additional ones, β_C for the average chirality below T_N and γ_C for the chiral susceptibility above T_N. This conjecture is still debated, as we believe, mainly due to the fact that until recently only the conventional exponents were the measured. We have concentrated on measurements of the chiral critical exponents that are evidently much more informative in studies of this type phase transitions. This become available with polarised neutron scattering. The critical behaviour of the average chirality, $\langle C\rangle \propto |\tau|^{\beta_C}$ can be obtained from the PD part of Eq. (16) if

$(n_R - n_L) \neq 0$. The chiral susceptibility is connected to four-spin correlations, which cannot be observed directly. We have investigated the dynamical chirality (DC), i.e., the projection of the chiral fluctuation field onto the magnetization induced by an external field [84]. The DC manifests itself in a completely inelastic PD part of the neutron cross-section [84, 85]. For a *XY* chiral antiferromagnet at $\omega << T$ it has been obtained [86] as an odd function of ω:

$$\left(\frac{d\sigma}{d\omega d\Omega}\right)_{\mathbf{P}_0} \approx A(\hat{\mathbf{Q}}\hat{\mathbf{h}})(\hat{\mathbf{Q}}\hat{\mathbf{c}})(\hat{\mathbf{c}}\hat{\mathbf{h}})\frac{\omega/\Gamma}{[1+(\omega/\Gamma)^2]^2}, \qquad (18)$$

where the scale factor A is a power function, $A \propto \tau^{-\phi_C}$, of the reduced temperature $\tau = (T - T_N)/T_N$, and $\phi_C = \beta_C + \gamma_C$ is the chiral crossover exponent. Eqs. (17), (18) allow the measuring of both chiral exponents, β_C and γ_C.

Using three crystals of a TLA $CsMnBr_3$ with the natural difference $(n_R - n_L) \approx 0.1$, we have obtained [87] as shown in Fig. 21 the average experimental value $\beta_C = 0.44(2)$ in agreement with the Monte Carlo value for the chiral-universality scenario [88] $\beta_C = 0.45(2)$. From the temperature dependence $A(\tau)$ shown in Fig. 22 the $\phi_C = 1.28(7)$ averaged over the fields $B = 4$ T and $B = 2$ T has been obtained for $\tau > 0.1$. (A crossover to $\phi_C \approx 0.2$ at $\tau < 0.1$ has been recently explained by a restricted momentum resolution [89].) From $\beta_C = 0.45(2)$ and $\phi_C = 1.28(7)$ one obtains $\gamma_C = \phi_C - \beta_C = 0.84(7)$ in agreement with the Monte Carlo result [88] $\gamma_C = 0.77(5)$. Our β_C and γ_C values together with the specific-heat exponent [90] $\alpha = 0.40(5)$

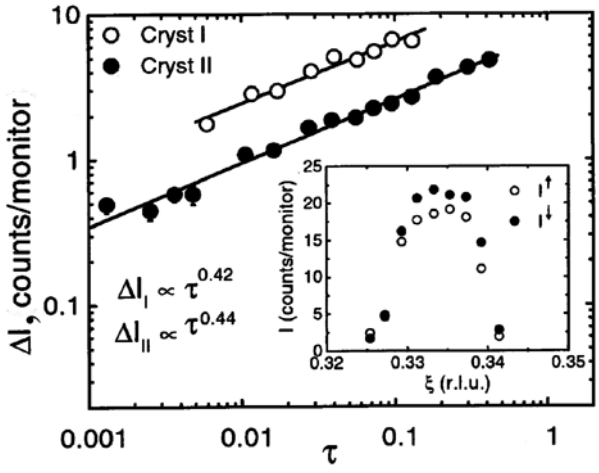

Fig. 21. The log-log plot of the PD intensity of the magnetic Bragg reflection (1/3, 1/3, 1) from two crystals of a TLA $CsMnBr_3$ *vs.* τ. The rocking curves with the opposite initial polarisation are shown

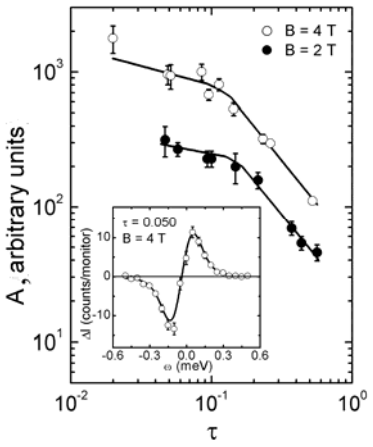

Fig. 22. The log-log plot of the scale factor A in Eq. (18) *vs.* τ at the position of the Bragg point (1/3, 1/3, 1) of the TLA $CsMnBr_3$. The inset shows an example of the energy depen-dence of the DC cross-section with the best fit by Eq. (18)

satisfy within error bars the scaling relation $\alpha + 2\beta_C + \gamma_C = 2$ expected from renormalization-group arguments [91]. In our case this sum is equal to 2.12(9). Our ability to disentangle the spin and chiral variables has allowed us to pursue the question of whether they are decoupled or not. The agreement between the chiral-order temperature and T_N within a relative precision of about 5×10^{-4} gives a strong support for the notion of a single, coupled order parameter, and all the data give for the first time evidence for the new chiral-universality class of a spin-order transition.

We have also studied the chiral criticality in the metallic holmium with the simple-spiral spin structure (Fig. 20 c, d). As mentioned above, the symmetry of the order parameter is the same as in $CsMnBr_3$, and therefore the spin-order transition should belong to the same chiral-universality class. However, the chiral criticality has occurred to be completely different [82]. The average chirality was determined from the inten-

sity difference, $\Delta = I^{\uparrow} - I^{\downarrow}$, of the first magnetic satellite (0, 0, μ) from the cylindrical crystal with the cylinder axis along [0, 0, 1]. To obtain a non-equal domain population the measurements were carried out under torsion deformation of about 2% around the cylinder axis. Unlike the previous case, the critical scattering as well as extinction were strong, and appropriate corrections of the experimental temperature dependences were made [82] as shown in Fig. 23.The final value of $\beta_C = 0.901(28)$ is twice as large in comparison with the Monte Carlo value [88] of $\beta_C = 0.45(2)$ and $\beta_C = 0.44(2)$ obtained in the experiment [87] for a TLA $CsMnBr_3$. Different from the situation studied in the Monte Carlo simulation, where the ordered ground state is characterized by a small finite number of spin orientations, in Ho the spin space is continuous in *xy*. This difference in the symmetry of the ground state could be an origin for the different critical exponents. Apparently the ratio of the correlation length and the interaction scale that determines the spiral pitch, or dipolar interaction between ferromagnetically ordered planes is important [92]. This also holds for comparison with $CsMnBr_3$. It is interesting that the chiral susceptibility exponent $\gamma_C = 0.68(5)$ obta-ined from β_C and ϕ_C (Fig 24), which characterizes the chiral fluctuations is not too far from the corresponding Monte Carlo [88] and experimental [87] values for a TLA $CsMnBr_3$, $\gamma_C = 0.77(5)$ and $\gamma_C = 0.84(7)$, respectively.

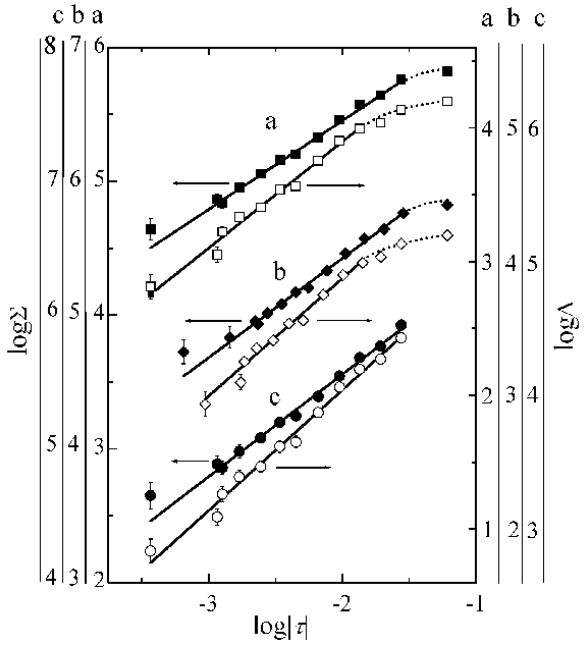

Fig. 23. The log-log plot of Σ and Δ *vs.* τ: (a), (b) critical scattering correction with $C^+/C^- = 2$ and $C^+/C^- = 5$, respectively; (c) correction for the critical scattering with $C^+/C^- = 2$, for the extinction and for the helix pitch

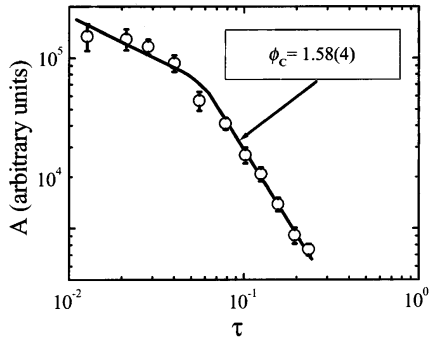

Fig. 24. Temperature dependence of the scale factor *A* in Eq. (18) for holmium

The exponent β_C has not to be necessarily equal to 2β as one could naively expect from Eq. (15). We have paid special attention to check whether $\beta_C = 2\beta$. Independently of the correction used (see Fig. 23) there is a stable difference of nearly four standard deviations. For the final result we take $\beta_C - 2\beta = 0.137(36)$ with a high reliability level. A possible explanation is that while β describes the critical behaviour of the longitudinal spin components S_z, β_C refers also to the correlations in the transverse components, which enter the thermal average of the vector product (15). This difference means that the chirality is an independent component of the order parameter.

8. *Miscelleneous*

Historically the second work after weak antiferromagnetism made using the polarisation analysis was a study of magnetic short range ordering in the rhombohedral β-phase ($23.9 < T$, K < 43.8) [93] and cubic γ-phase ($43.8 < T$, K < 54.4) of solid oxygen [94]. The difference of the spin-flip scattering with the polarisation along the scattering vector and the polarisation vertical that gives 1/3 of the purely magnetic cross-section has allowed measuring very weak magnetic signal. The O_2 spins ($S = 1$), which have a collinear antiferromagnetic long-range structure in the low temperature monoclinic α-phase (T < 23.9 K) [95], show in the

β-phase a two-dimensional short range order, a helix propagating perpendicular to the three fold axis with an angle of 141º between the nearest molecules and with a correlation length of about 5 Å. In the solid high temperature γ-phase only the antiferromagnetic correlation $\langle \mathbf{S}_1\mathbf{S}_2 \rangle = -0.90(7)$ between the nearest molecules in the chain along a [1, 0, 0] direction has been found. The spin is found to be perpendicular to the molecular axis. Similar antiferromagnetic fluctuations have been observed in the liquid [94] and even in the dense gas, which indicates the dependence of the oxygen-oxygen scattering cross-section on the mutual molecular spin orientation. These investigations were used in the thesis of F. Dunstetter (Saclay, France).

On the early age of the high-T_C superconductivity the YBCO–type materials with the general formula $R\mathrm{Ba_2Cu_3O_{6+x}}$ (R is Y or a rare earth) were the most popular. Therefore, the triangle $R_2O_3 - CuO_2 - BaO$ was investigated in detail when searching for the materials with the highest T_C. These investigations resulted in a series of new phases, which had no superconductivity but possessed very interesting magnetic proper-ties. Having a powder diffractometer with a quite good resolution and luminosity as well as experience in the profile analysis of the powder neutron diffraction data and in the group-symmetry analysis of the magnetic structures, we investigated magnetic ordering in a number of these materials [96 – 98]. The first series studied is so-called "green phase" with the orthorhombic structure that is almost inevitable at the synthesis of the YBCO–type systems. Very unusual for the rare-earth oxides is magnetic ordering of the rare-earth subsystem simultaneously with the copper subsystem at rather high temperature ~ 10 K. (Normally the ordered spins of 3*d*-ions polarize the rare-earth ions, the magnetic moments of which order at very low temperature ~ 1 K.) For the compounds of Y, Dy, Ho, Er, Tm, Yb and Gd studieda variety of magnetic structures was observed with the wave vectors [0,0,0], [0,1/2,0], [0,0,1/2], [0, 1/2,1/2]. An example of arrangement of the Cu^{2+} and the R^{3+} moments in one chemical cell is given in Fig. 25 for Er_2BaCuO_3. The spin-reorientation transitions are observed in Dy_2BaCuO_3 and Ho_2BaCuO_3.

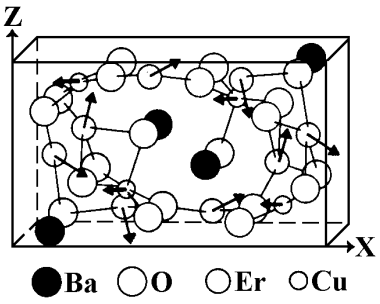

Fig. 25. Arrangement of magnetic moments (Cu^{2+} and Er^{3+}) in the chemical unit cell of Er_2BaCuO_5. Magnetic wave vector $\mathbf{k} = (\pi/b)$ [0,1,0] reverses all the moments in the nearest cell along **y**

Another series of compounds with the general formula $R_2Cu_2O_5$ (R = Lu, Er, Tb, Tm, Ho, Dy) and with orthorhombic structure, so-called "blue phase" was investigated in Refs. [99 – 102]. In these materials there are the layers perpendicular to the [0,0,1] direction, in which the Cu^{2+} ions have double superexchange bonds Cu-O-Cu with the bond angle is close to 90º. As a result the copper spins in these layers are ordered ferromagnetically. Again the rare-earth and copper moments order simultaneously at $T_N \sim 10 \div 20$ K, which is unusually high temperature for the rare earths. Unlike the copper spins ordered ferromagnetically in the layers and antiferromagnetically between the layers, the rare-earth moments are not collinear. In some compounds an additional magnetic transition, apparently due to the spin reorientation, was observed.

A lanthanum-copper oxide with the same formula $La_2Cu_2O_5$ as the previous series, but with completely different monoclinic structure has been studied by the single crystal neutron diffraction. The atomic positions and the spin ordering are determined [103]. This material contains distorted blocks of La_2CuO_4, and like the latter shows a low-dimensional magnetic behaviour with critical index $\beta = 0.228(8)$.

The intermetallic rare-earth compounds RM_2 have been studied, with the properties that are governed by magnetic instability and frustration in M-sublattice. The instability of 4*f*-electrons is investigated in $TmCo_2$ and is explained by a critical interatomic distance in the region of homogeneity [104, 105]. If M stands for Mn the character of 3*d*-electrons can be changed between itinerant and localized when the Mn-Mn spacing is varied. The substitution of Mn by Al increases this spacing, which allows approaching the instability region in $Ho(Mn, Al)_2$. Our experiments show the coexistence of phases with incommensurate and ferromagnetic order in this system that is attained to the dominant role of spontaneous Mn-moment [106]. The substitution in the $Dy(Mn, Al)_2$ system allows to encompass the instability threshold and to observe new effects.

Neutron diffraction studies of magnetism in restricted geometry of the nanometer-scale pores have been started. The first systematic investigation of a magnet embedded in a porous glass carried out with antiferro-

magnetic MnO has shown a diversity of finite-size effects [107]. Similar experiments with ferromagnetic Fe and Ni have shown the thermal expansion coefficients to be essentially smaller than in the bulk. From the diffraction peak broadening an appearance of the inner strains is found.

A series of the X-ray works [108-111] have been devoted to the experimental prove of a concept [112] of the cooperative thermal motion in crystals (metals, compounds, ionic crystals etc.). For the first time a quantitative analysis of the thermal diffuse X-ray scattering has been carried out that allows determining the values of theoretical parameters, ζ, describing the dynamical correlations of atoms in a highly symmetrical ideal crystal. The correlation parameters obtained from the experiment change with the temperature in accordance with theoretical predictions [111]. In the case of the $Ni_{51}Ti_{49}$ alloy the diffuse rods and planes are observed in the reciprocal space at high temperature. Their width is decreasing down to the instrumental resolution at the temperature T_s of structural phase transition. The value ζ is determined from the peak width. The number of the unit cells with correlated atomic movement increases from $3 \div 4$ at high temperature up to about 100 near T_s.

X-ray diffuse scattering studies are carried out on single crystals of the electro-technical steel Fe-Si with low silicon content [113]. The 50 years-old Néel hypothesis on the oriented ordering of Si atoms caused by a thermomagnetic treatment (TMM) is experimentally proved. This means that an improvement of the steel after the TMT is connected with the crystalline anisotropy.

Epilogue

39 years have passed since the first experiment that can be considered as a property of our laboratory. We started from zero, having no experience, no instruments and no actual money for the instrumentation. Nevertheless we have designed 3 neutron scattering instruments that work now at the WWR-M reactor and two X-ray instruments, one of which can be used for the neutron diffraction. Because of the lack of the money everything is homemade.

Starting from the neutron powder diffraction, we have got experience in the other neutron methods including inelastic scattering, and all kinds of the polarized neutron scattering. The polarisation analysis technique made 24 years ago was that time on the level of high-flux reactors. Now our luminosity is at least two orders of magnitude lower than at any ILL spectrometer, where new focusing crystals with the area of about 20×20 cm^2 are used. All the inelastic neutron scattering experiments were made at the triple axis spectrometers of *Institut Laue-Langevin*. I tried to get a triple axis spectrometer in seventies, but always failed to find the money. A homemade version of such an instrument seems to be not very realistic.

X-ray scattering has been included in the area of our interest, and a number of experiments are performed with the synchrotron X-rays at NSLS (Brookhaven, USA), LURE (Orsay, France), ESRF (Grenoble, France), DASYLAB (Hamburg, Germany), Brazilian Synchrotron Centre.

About 30 people went through our laboratory during all these years, but the size of this organism was never more than 15 persons altogether. As a result of scientific activity reviewed in the previous sections, a number of colleagues have defended the thesis:

1. I. V. Golosovsky – Spin structures of the antiferromagnetic garnets.
2. Yu.P. Chernenkov – Weak antiferromagnetism and anisotropic interactions in the rare-earth orthoferrites.
3. A.V. Kovalev – Structural and magnetic phase transitions in the ferroelectric boracites.
4. O.P. Smirnov – Neutron diffraction and computer simulation studies of magnetically diluted garnets.
5. I.A. Zobkalo – Polarized neutron scattering and investigation of magnetic properties of compounds R_2CuO_4 (R = La, Sr, Nd, Ce, Eu, Sm, Gd).
6. A.B. Stratilatov – X-ray studies of the oxygen ordering in the high-T_C system $YBa_2Cu_3O_{6+x}$.
7. V.G. Galushko (PTI, Donetzk) – Weak antiferromagnetism and spin-flop transition in $CuCl_2 \cdot 2D_2O$.
8. F. Dunstetter (Saclay, France) – Magnetic correlations in the β- and γ-phases of solid oxygen.
9. F. Yakhou (J. Fourier University, Grenoble, France) – Discovery, identification and the structure determination of the epitaxy compound Ba_3CuO_4.

Crystal Physics Laboratory (Department for Condenced-Matter Investigation, Neutron Studies Division)
on the salary-payment day, Friday, the 8th of June 2001.
From the left to right standing: V.I. Fedorov, S.V. Gavrilov, O.P. Smirnov, E.V. Moskvin, V.A. Polyakov, Yu.P. Chernenkov, I.A. Zobkalo, A.M. Golubev, I.V. Golosovsky; sitting V.I. Smurov, P.A. Karnayeva, V.P. Plakhty, E.I. Fedorova

At present our laboratory consists of 13 persons together with the boss (see photo). It includes three generations of the neutron scatterrers, from the second to the fourth. (I consider myself as a representative of the second generation.) "With a little help from our friends" and from *Ministère d'Éducation Supérieur et de Recherche Française*, where we have got a grant for young people, almost all the members of the laboratory have had long-term stays (up to one and a half years) in Grenoble. As a result, all the physicists are experienced in several neutron methods that were used during their stay and during numerous short-term experiments made on various instruments at the reactor SILOË, *Commisariat d'Energy Atomique* – Grenoble) and at the high-flux reactor of *Institut Laue-Langevin*. This means that, in principle, the team can carry out now investigations that need any neutron scattering method. This is very good since we can make successful proposals for the ILL instruments and perform an experiment that we need to solve a physical problem, independently of what is available in our laboratory at our own reactor. On the other hand this is very bad because the youngest generation becomes accustomed to use a working instrument just playing on the keyboard. Very long and uneasy stage of designing and construction of the own instrument is missed in their education. An organism like laboratory has to have its own equipment that should offer better possibilities than the other people have (see preface), even in such a pleasant place as Grenoble.

First of all we need a high flux in the core. The PIK reactor story is rather sad, but recently some very important positive changes have happened as to my knowledge. Very important are the modern instruments, which can improve the experimental conditions much more than the high flux itself. The experience, our colleagues have got being "casted away", has to be used now to improve existing instruments and to design the new ones of a real quality.

"For everything there is a season, and a time for every matter under heaven:
a time to cast away stones, and a time to gather stones together" [114].

During our life we have gone as far as a pitch of the spiral to come to the starting point in the transverse coordinates. Again as at the very beginning we have to make a plenty of machinery with no money. But the pitch is passed, and this time we know at least more Words how to "do neutrons". Let us "gather stones together."

REFERENCES

[1] John, chapter 1, verse 1 - *The New Oxford Annotated Bible* (1977) p.1286.
[2] V.P. Plakhty, E.I. Maltzev, D.M. Kaminker, Izv. Akad. Nauk SSSR, ser.fiz. **28,** 436 (1964).
[3] V. Plakhty, W. Cochran, Phys. stat. solidi **29**, K81 (1968).
[4] E.F. Bertaut F. Forrat, A. Herpin, P. Meriel, C.R. **243**, 898 (1956).
[5] V. Plakhty, I. Golosovsky, V. Kudryashev, N. Parfenova, O. Smirnov, Pis'ma v ZhETF **18**, 85 (1973) [JETP Lett. **18** (1973)].
[6] S.R. Broadbent and J.M. Hammersley, Proc. Cambridge Phil. Soc. **53**, 629 (1957).
[7] C. Domb and M.F. Sykes, Phys. Rev. **122**, 77 (1961).
[8] Yu.A. Izyumov, V.E. Naish, and R.P. Ozerov. Neutron diffraction of magnetic materials. New York & London: Consultants Bureau, 1991.
[9] V.P. Plakhty, I.V. Golosovsky, M.N. Bedrizova, O.P. Smirnov, V.I. Sokolov, B.V. Mill, N.N. Parfenova, Phys. stat. solidi (a) **39**, 683 (1977); V.P. Plakhty, I.V. Golosovsky, Phys. stat. solidi (b) **53**, K37 (1972).
[10] R. Plumier, Solid State Commun. **10**, 5 (1972); W. Prandl, *ibid* **10**, 529 (1972).
[11] V. Plakhty, I. Golosovsky, Sov. Phys. Solid State **14**, 2387 (1973).
[12] W. Prandl, Solid State Commun. **11**, 645 (1972).
[13] K.P. Belov, B.V. Mill, V.I. Sokolov, O.I. Shevaleevsky, Sov. Phys. JETP Lett. **20**, 42 (1974).
[14] V.I. Sokolov, O.I. Shevaleevsky, Sov. Phys. JETP **45**, 1245 (1977).
[15] Th. Brueckel, B. Dorner, A.G. Gukasov, V.P. Plakhty, W. Prandl, E.F. Shender, and O.P. Smirnov, Z. Phys. B – Condensed Matter **72**, 477 (1988).
[16] Th. Brueckel, Yu. Chernenkov, B. Dorner, V.P. Plakhty, and O.P. Smirnov, Z. Phys. B – Condensed Matter **79**, 389 (1990).
[17] V. Plakhty, I. Golosovsky, A. Gukasov, O. Smirnov, Th. Brueckel, B. Dorner, P. Burlet, Z. Phys. **B 92**, 443 (1993).
[18] J. Hubbard and W. Marshall, Proc. Phys. Soc. **86**, 561 (1965).
[19] V.P. Plakhty, A.G. Gukasov, R.J. Papoular and O.P. Smirnov, Europhys. Lett. **48**, 233 (1999).
[20] K.P. Belov, and V.I. Sokolov, Sov. Phys. Usp. **20**, 149 (1977).
[21] E. Shender, Sov. Phys. JETP **56**, 178 (1982).
[22] I.E. Dzyaloshinsky, ZhETF **32**, 1547 (1957), in Russian.
[23] T. Moriya, Phys. Rev. **120**, 91 (1960).
[24] A.S. Borovik-Romanov, M.P. Orlova, ZhETF **31**, 579 (1956); A.S. Borovik-Romanov, *ibid* **36**, 766 (1959); A.S. Borovik-Romanov, V.I. Ozhogin, *ibid* **39**, 27 (1960).
[25] H. Umebayashi, B.C. Frazer, D.E. Cox, G. Shirane, Phys. Rev. **167**, 519 (1968).
[26] V.P. Plakhty, Yu.P. Chernenkov, J. Schweizer, M.N. Bedrizova, Sov. Phys. JETP **53**, 1291 (1981).
[27] V.P. Plakhty, Yu.P. Chernenkov, M.N. Bedrizova, J. Schweizer, In "Neutron Scattering", Symp. Argonne, III, 1981. New York (1982) p.330.
[28] V.P. Plakhty, Yu.P. Chernenkov, M.N. Bedrizova, Solid State Commun. **47**, 309 (1983).
[29] S.M. Shapiro, J.D.Axe, J.P. Remeika, Phys. Rev. **B 10**, 2014 (1974).
[30], E.A.Turov, V.E. Naush, Phys. Met. Metallogr. **9**, 10 (1960), in Russian.
[31] A.S. Moskvin, E.V. Sinitzin, Fiz. Tverd. Tela **14**, 2535 (1972); A.S. Moskvin, I.G. Bostrem*, ibid* **19**, 1616 (1977) – in Russian.
[32] Yu.P. Chernenkov, V.P. Plakhty, A.V. Kovalev, Preprint LNPI– 897, L., 1983, 25 p., in Russian.
[33] T.A. Kaplan, Phys. Rev. **136**, 1634 (1964).
[34] V.P. Plakhty, A.V. Kovalev, M.N. Bedrizova, Yu.P. Chernenkov, B.A. Galushko, V.T. Telepa, Preprint LNPI– 809, L., 1982, 36 p.
[35] V. Plakhty, Solid State Commun.**79**, 313 (1991).
[36] E. Buluggiu, G.Dascola, D.C. Vera, J. Chem. Phys. **54**, 2191 (1971).
[37] G.M. Drabkin, E.I. Maltzev, V.P. Plakhty, Fiz. Tverd. Tela **7**, 1241 (1965), in Russian.
[38] G.A. Smolensky, V.A. Bokov, S.A. Kizhaev, E.I. Maltzev, G.M. Nedlin, V.P. Plakhty, A.G. Tutov, V.M. Judin, *In:Proc. Int. Conf. Magnetism*. Nottingham, 1964, p.354.
[39] G. Rado, Phys. Rev. Lett. **11**, 609 (1961).
[40] M. Date, J. Kanamori, M. Tanaki, J. Phys. Soc. Jpn. **16**, 2589 (1961).

[41] T. Ito, N. Marimoto, R. Sadanaga, Acta Cryst. **4**, 310 (1954).
[42] A.V. Kovalev, V.P. Plakhty, G.T. Andreyeva, Sov. Fiz. Tverd. Tela **19**, 1179 (1977). [Phys. Solid State **19**, N°4 (1977)].
[43] V. Plakhty, A. Kovalev, M. Bedrizova, I. Golosovsky, G. Andreeva, Fiz. Tverd. Tela **18**, 2030 (1976).
[44] A. Kovalev, V. Plakhty, G. Andreeva, JETP Lett. **27**, 637 (1978).
[45] E.I. Golovenchits, N.V. Morozov, V.A. Sanina, L.M. Sapozhnikova, Sov. Phys. Solid State **34**, 56 (1992).
[46] H. Tsujino, K. Kohn, Solid State Commun. **83**, 639 (1992).
[47] T. Doi, K. Kohn, Phase Transitions **38**, 273 (1992).
[48] K. Saito, K. Kohn, J. Phys.: Condens. Matter **7**, 2855 (1995).
[49] V. Polyakov, V. Plakhty, M. Bonnet, P. Burlet, L.-P. Regnault, S. Gavrilov, I. Zobkalo, O. Smirnov, Phys. **B 297**, 208 (2001).
[50] E.V. Enevskaya, A.M. Golubev, A.M. Kachurin, A.N. Savel'ev and K. N. Neustroev, Carbohydr. Res. **305**, 83 (1998).
[51] A.M. Kachurin, A.M. Golubev, M.M. Geisow,O.S. Veselkina and L.S. Isaeva-Ivanova, Biochem. J **308**, 955 (1995).
[52] A.M. Golubev, J.R. Brandão Neto, E.V. Enevskaya, A.V. Kulminskaya, M.A. Kerzhner, K.N. Neustroev and I. Polikarpov, Acta Cryst. **D 56**, 1058 (2000).
[53] R. Aparicio, E.V. Enevskaya, A.A. Kulminskaya, A.N. Savel'ev, A.M. Golubev, K.N. Neustroev, J. Kobarg and I. Polikarpov, Acta Cryst. **D 56**, 342 (2000).
[54] A.G. Gukasiv, V.P. Plakhty, V.A. Polyakov, I.A. Zobkalo, Physica **B 180-181**, 1007 (1992).
[55] R,J. Cava, A.W. Hewat, B. Batlog, M. Merezio, K.M. Rabe, W.F. Krajevski, W.F. Peck and L.W. Rupp, Physica **C 165**, 419 (1990).
[56] J. Jorgensen, B.W. Veal, A.P. Paulikas, L.J. Novicki, G.W. Crabtree and W.K. Kwok, Phys. Rev. **B 41**, 1863 (1990).
[57] G. Uimin, J. Rissat-Mignod, Physica **C 199**, 251 (1992).
[58] Yu. A. Osipyan, O.V. Zharikov, H.C. Sidorov et al. Pis'ma v ZhETF **48**, 225 (1988), in Russian.
[59] Yu. Osip'an, E. Bokhenkov, I. Golosovsky, O. Zharikov, A. Krasheninnikov, S. Kuznetsov, R. Nikolaev, V. Plakhty, E. Ponyatovsky et al. JETP Lett. **49** (1989) 248.
[60] V. Plakhty, A. Stratilatov, Yu. Chernenkov, V. Fedorov, S.K. Sinha, Chun K. Loong, B. Gaulin, M. Vlasov and S. Moshkin, Solid State Commun**. 84**, 639 (1992).
[61] V. Plakhty, B. Kviatkovsky, A. Stratilatov, Yu. Chernenkov, P. Burlet, J.Y. Henry, C. Marin, E. Ressouche, J. Schweizer, F. Yakhou, E. Elkaim, J.P. Lauriat, Physica **C 235 –240**, 867 (1994).
[62] P. Burlet, V. Plakhty, C. Marin, J.Y. Henry, Phys. Lett. **A 167**, 401 (1992).
[63] A. Stratilatov, V. Plakhty, Yu. Chernenkov and V. Fedorov, Phys. Lett. **A 180**, 137 (1993).
[64] V. Plakhty, P. Burlet, J.Y. Henry, Phys. Lett. **A 198**, 256 (1995).
[65] D. de Fontaine, G. Ceder and M. Asta, Nature 343, 544 (1990).
[66] M.A. Alario-Franco, C. Chaillout, J.J. Capponi, J. Chenavas, M. Marezio, Physica **C 156**, 455 (1988).
[67] R. Sonntag, D. Hohlwein, Th. Brueckel, G. Collin, Phys. Rev. Lett. **66**, 1497 (1991).
[68] F. Yakhou, V. Plakhty, G. Uimin, P. Burlet, B. Kvyatkovsky, J.Y. Henry, J.P. Lauriat, E. Elkaim, E. Ressouche, Solid State Commun. **94**, 695 (1995).
[69] F. Yakhou, V. Plakhty, A. Stratilatov, P. Burlet, J.P. Lauriat, E. Elkaim, J.Y. Henry, M. Vlasov, S. Moshkin, Physica **C 261**, 315 (1996).
[70] R.J. Birgenau, Y. Endoh, G. Shirane et al. Phys. Rev. **B 38**, 6614 (1988).
[71] A.G. Gukasov, V.P. Plakhty, I.A. Zobkalo et al. Mater. Science Forum **62-64**, 187 (1990).
[72] A.G. Gukasov, S.Yu. Kokovin, V.P. Plakhty, I.A. Zobkalo, S.N. Barilo and D.I. Zhigunov, Physica **B 180-181**, 455 (1992)
[73] T. Chattopadhayay, P.J. Brown, I.A. Zobkalo et al. Phys.Rev. **B** 44, 9486 (1991).
[74] A.G. Gukasov, V.A. Polyakov, I.A. Zobkalo, D. Petitgrand, P. Burges, L. Budarèn, S.N. Barilo, D.N. Gigunov, Solid State Commun. **95**, 533 (1995).
[75] D. Petitgrand, A.H. Moiden, P. Galoz, P. Boutroille, J. Less Common Metals **164-165**, 768 (1990).
[76] I.W. Sumarlin, J.W. Lynn, T. Chattopadhyay, S.N. Barilo, D.I. Zhigunov, J.L. Peng, Phys. Rev. **B 51**, 5824 (1995).
[77] D. Petitgrand, S.V. Maleyev, Ph. Bourges, A.S. Ivanov, Phys. Rev. **B 59**, 1079 (1999).
[78] S.T. Balayev, Sov. Phys. JETP **7**, 299 (1958).
[79] O.L. Zhizhimov and I.B. Khriplovich, ZhETF **84**, 342 (1983), in Russian.
[80] S.V. Maleyev, V.G. Bar'yakhtar, and R.A. Suris, Fiz. Tver. Tela **4**, 3461 (1962), in Russian, [Sov. Phys, Solid State **4**, 2533(1963)]; Yu.A. Izyumov, ZhETF **43**, 1673 (1962), in Russian; M. Blume, Phys. Rev. **130**, 1670 (1963).
[81] V.I. Fedorov, A.G. Gukasov, V. Kozlov, S.V. Maleyev, V.P. Plakhty, Phys. Lett. **A 224**, 372 (1997).
[82] V.P. Plakhty, W. Schweika, Th. Brückel, J. Kulda, S.V. Gavrilov, L.-P. Regnault and D. Visser, Phys . Rev. **B** – in press.
[83] J. Kawamura, J. Phys. Condens. Matter **10**, 4707 (1998)
[84] S.V. Maleyev, Phys. Rev. Lett. **75**, 4682 (1995).
[85] S.V. Maleyev, V.P. Plakhty, O.P. Smirnov, J. Wosnitza, D. Visser, R.K. Kremer and J. Kulda, J. Phys.: Condens. Matter **10**, 951 (1998).
[86] V.P. Plakhty, S.V. Maleyev, J. Kulda, J. Wosnitza, D. Visser and E. Moskvin, Europhys. Lett. **48**, 215 (1999).
[87] V.P. Plakhty, J. Kulda, D. Visser, E.V. Moskvin and J. Wosnitza, Phys. Rev. Lett. **85**, 3942 (2000).
[88] H. Kawamura, J. Phys. Soc. Jpn. **61**, 1299 (1992).
[89] S.V. Maleyev, Usp. Fiz. Nauk (2001) – in press.
[90] R. Deutschmann, H. v. Löhneysen, J. Wosnitza, R.K. Kremer and D. Visser, Europhys. Lett. **17**, 637 (1992).
[91] H. Kawamura, Phys. Rev. **B 38**, 4916 (1988); J. Phys. Soc. Jpn. **59**, 2305 (1990).
[92] J. Wang, D.P. Belanger and B.D. Gaulin, Phys. Rev. Lett. **66**, 3195 (1991)
[93] F. Dunstetter, V. Plakhty, J. Schweizer, J. Magn. Mag. Mat. **72**, 258 (1988).

[94] F.Dunstetter, V. Plakhty, J. Schweizer, J. Magn. Mag. Mat. **96**, 282 (1991).
[95] R.A. Alikhanov, JETP Lett. **5**, 349 (1967).
[96] I. Golosovsky, V. Plakhty, V. Kharchenkov, Ya. Zoubkova, B. Mill, M. Bonnet, E. Roudaut, Sov. Phys. Solid State **34** (1992) 782.
[97] I.V. Golosovsky, P. Böni and P. Fischer, LNS ETHZ & PSI Progress Report, 110 (1992).
[98] I.V. Golosovsky, P. Böni and P. Fischer, Solid State Commun. **87**, 1473 (1993).
[99] V.P. Plakhty, I.V. Golosovsky, J. Zoubkova, S.A. Kuznetsov, B.V. Mill and V.P. Harchenkov, JETP Lett. **51**, 54 (1990).
[100] V.P. Plakhty, M. Bonnet, I.V. Golosovsky, B.V. Mill, E. Roudeau and E.I. Fedorova, JETP Lett. **51**, 725 (1990).
[101] I. Golosovsky, B. Mill, V. Plakhty, V.Kharchenkov, Fiz. Tverd. Tela **33**, 3412 (1991) [Sov.Phys. Solid State **33** (1991)].
[102] I.V. Golosovsky, V.P. Plakhty, V.P. Harchenkov, S.V. Sharygin and J. Schweizer, J. Magn. Mag. Mat. **129**, 233 (1994).
[103] I.V. Golosovsky, A.G. Gukasov, V.A. Polyakov, D.I. Zhigunov and I.A. Zobkalo, J. Phys.: Condens. Matter **11**, 6958 (1999).
[104] I. Dubenko, I. Golosovsky, E. Gratz, R. Levitin, A. Markosyan and S. Sharygin, J. Magn. Mag. Mat. **150**, 304 (1995).
[105] I. Golosovsky, B. Kvyatkovsky, S. Sharygin, I. Dubenko, R. Levitin, A. Markosyan, E. Gratz, I. Mirebeau, I. Goncharenko and F. Bourée, J. Magn. Mag. Mat. **169**, 123 (1997).
[106] I. Dubenko, I. Golosovsky, A. Markosyan and I. Mirebeau, J. Phys.: Condens. Matter. **10**, 11755 (1998).
[107] I. Golosovsky, I. Mrebeeau, G. Andre, D. Kurdyukov, Yu. Kamzerov and S. Vakhrushev, Phys. Rev. Lett. **86**, 5783 (2001).
[108] V.E. Naish, T.V. Novoselova, I.V. Sagaradze, V.I. Fedorov, Yu.P. Chernenkov, Phys. Met. Metallogr. **77**, 472 (1994).
[109] V.E. Naish, T.V. Novoselova, I.V. Sagaradze, V.I. Fedorov, B.E. Kvyatkovsky, Yu.P. Chernenkov, Phys. Met. Metallogr. **77**, 479 (1994).
[110] V.E. Naish, T.V. Novoselova, I.V. Sagaradze, V.I. Fedorov, Yu.P. Chernenkov, Phys. Met. Metallogr. **79**, 291 (1995).
[111] V.E. Naish, T.V. Novoselova, V.G. Pushin, I.V. Sagaradze, V.I. Fedorov, Yu.P. Chernenkov, Phys. Met. Metallogr. **81,** 6 (1995).
[112] F.A. Kassan-Ogly, V.E. Naish, I.V. Sagaradze, Phase Transitions **49**, 89 (1994).
[113] Yu. P. Chernenkov, V.I. Fedorov, V.A. Lukshina, B.K. Sokolov, N.V Ershov, Phys. Met. Metallogr. (2001) – in press.
[114] Ecclesiates, chapter 3, verses 1, 5 – *The New Oxford Annotated Bible* (1977) p. 807.